Rapid Assembly of Infection Resistant Coatings: Screening and Identification of Antimicrobial Peptides Works in Cooperation with an Antifouling Background

Journal:	*ACS Applied Materials & Interfaces*
Manuscript ID	am-2021-07515u.R3
Manuscript Type:	Article
Date Submitted by the Author:	n/a
Complete List of Authors:	Yu, Kai; The University of British Columbia, Pathology and Lab Medicine Alzahrani, Amal ; The University of British Columbia, Department of Urologic Sciences Khoddami, Sara; The University of British Columbia, Department of Urologic Sciences Cheng, John; Simon Fraser University, Physics Mei, Yan; University of British Columbia, Department of Pathology and Laboratory Medicine Gill, Arshdeep; The University of British Columbia, Chemistry Luo, Haiming; The University of British Columbia Faculty of Science Haney, Evan; University of British Columbia, Microbiology and Immunology Hilpert, Kai; University of London Saint George's, Infection and Immunology Research Institute Hancock, Robert; University of British Columbia, Centre for Microbial Diseases & Immunity Research Lange, Dirk; University of British Columbia, Urologic Sciences Kizhakkedathu, Jayachandran; University of British Columbia, Department of Pathology and Lab Med. & Center for Blood Research

Rapid Assembly of Infection Resistant Coatings: Screening and Identification of Antimicrobial Peptides Works in Cooperation with an Antifouling Background

Kai Yu,[1] Amal Alzahrani,[2] Sara Khoddami,[2]John T. J. Cheng,[3] Yan Mei,[1] Arshdeep Gill,[4] Haiming D. Luo,[4] Evan F. Haney,[3] Kai Hilpert,[5] Robert E.W. Hancock,[3] Dirk Lange[2]* and Jayachandran N. Kizhakkedathu[1,4,6]*

[1]Centre for Blood Research and Department of Pathology & Laboratory Medicine, University of British Columbia, Vancouver, British Columbia V6T 1Z3, Canada. [2] The Stone Centre at VGH, Department of Urologic Sciences, University of British Columbia, Vancouver, British Columbia V5Z 1M9, Canada. [3]Department of Microbiology and Immunology and Centre for Microbial Diseases and Immunity Research, University of British Columbia, Vancouver, British Columbia V6T 1Z4, Canada.[4]Department of Chemistry, University of British Columbia, Vancouver, British Columbia V6T 1Z3, Canada. [5]Institute of Infection and Immunology, St. George's University of London (SGUL), London, United Kingdom. [6]The school of biomedical engineering, University of British Columbia, Vancouver, British Columbia, V6T 1Z3, Canada.

*to whom correspondence should be addressed.

Dr. Jayachandran N Kizhakkedathu

Department of Pathology and Laboratory Medicine,

Centre for Blood Research,

University of British Columbia

Email: jay@pathology.ubc.ca

or

Dr. Dirk Lange

Email: dirk.lange@ubc.ca

Department of Urological Sciences

Abstract

Bacterial adhesion and the succeeding biofilm formation onto surfaces are responsible for implant and device associated infections. Bifunctional coatings integrating both non-fouling components and antimicrobial peptides (AMPs) are a promising approach to develop potent antibiofilm coatings. However, the current approaches and chemistry for such coatings are time-consuming and dependent on substrates, and involve multi-step process. Also, the information is limited on the influence of the coating structure or its components on the antibiofilm activity of such AMP-based coatings. Here, we report a new strategy to rapidly assemble a stable, potent and substrate-independent AMP based antibiofilm coating in a non-fouling background. The coating structure allowed for the screening of AMPs in a relevant non-fouling background to identify optimal peptide combinations that work in cooperation to generate potent antibiofilm activity. The structure of the coating was changed by altering the organization of the hydrophilic polymer chains within the coatings. The coatings were thoroughly characterized using various surface analytical techniques and correlated with the efficiency to prevent biofilm formation against diverse bacteria. The coating method that allowed the conjugation of AMPs without altering the steric protection ability of hydrophilic polymer structure results in a bifunctional surface coating with excellent antibiofilm activity. In contrast, the conjugation of AMPs directly to the hydrophilic polymer chains resulted in a surface with poor antibiofilm activity and increased adhesion of bacteria. Using this coating approach, we further established a new screening method and identified a set of potent surface tethered AMPs with high activity. The success of this new peptide screening and coating method is demonstrated using a clinically relevant mouse infection model to prevent catheter associated urinary tract infection (CAUTI).

Keywords: Antibiofilm coating, Substrate independent coating, Implant associated infection, Antimicrobial peptides, Screening method, Bifunctional coating

1. Introduction

Medical devices have transformed the modern healthcare and evidences support the fact that its use helped to improve the quality of life for those living with serious injuries and chronic diseases. While these devices are necessary, the introduction of a foreign material into the body unavoidably sets the stage for potential microbial colonization and infection. This is evidenced by the ever-growing number of indwelling device-associated infections which account for 50-70% of the nearly 2 million healthcare-associated infections reported by the Center for Disease Control in the United States.[1-2] The opportunistic biofilm-forming pathogens can cause severe infections and, in some cases, death, particularly in patients with compromised immune system.[3] A recent estimate from United States showed that medical device-associated infections cause approximately 82,000 deaths/year and costs around $18 billion to the healthcare.[4] This prompted the search for preventative strategies to address this difficult challenge. Various approaches are currently being investigated to prevent implant/device associated infections, and the most promising ones include that prevent bacterial colonization and biofilm formation. Anti-adhesive and surface coatings that kills bacteria have shown great promise to combat device/implant infections.[5-12] There are several configurations or structures that have been adopted in the literature, including combining biocidal sub-layers with antifouling outer layers,[5-6] contact-active antimicrobial upper-layers and antifouling sub-layers[7-8] and, layering evenly mixed antimicrobial and non-fouling components.[9-12] Such surfaces are designed with a goal to achieve both the killing of bacteria owing to the presence of antimicrobial component and the prevention of bacterial adhesion (dead or live) due to the presence of the non-fouling component, to realize the overall antibiofilm efficacy. While the idea of dual functional coatings is not new, their adaptation is limited by the complicated synthesis protocols including the need for multiple chemical modifications.[5-19] As a result, previously proposed approaches are not an ideal platform to optimize the antimicrobial/antifouling efficiency.

With regards to antimicrobial agents, coatings containing covalently attached antimicrobial peptides (AMPs) showed excellent ability in preventing implant-associated infections in mouse models.[11-14] AMPs have broad spectrum antibiofilm activity and minimal chance of developing resistance due to their mode of action on bacterial membranes. However, tethered AMPs often showed decreased activity when compared to their soluble forms,[15] which limits the efficient biofilm prevention by most peptides. The conjugation methods also influence the antimicrobial and antibiofilm activities of surface immobilized peptides since tethering impact on their mobility and flexibility.[15-19] Most often, the conjugation is dependent on the substrate (various biomedical plastics, metals, ceramics, hydrogels etc.), and multiple modification steps (and chemistry) are needed to achieve a stable AMP-based coating on the surface.[14-19]

With respect to AMP selection, previous AMP screening studies to identify surface-tethered AMPs have been built on different solid substrates that did not account for non-specific adhesion of bacteria which can foul the surface.[20-22] In these methods, the AMPs were tethered with an intent to maximize the peptide density, which can easily be overwhelmed by higher planktonic bacterial concentrations resulting in fouling of the surface by dead or live bacteria[14-15,23-25] or fouling agents present in complex biological environment. The short-term activity readouts from different assays used in these approaches are thus not a true measure of their long-term activity. Having AMPs attached in a non-fouling background has the potential to manifest peptide activity in an uncompromised manner with a greater possibility for success when translated as an implant/device coating. But the current synthesis methods do not allow for rapid generation of such non-fouling coating for screening of potent surface-tethered AMPs.

Polydopamine-based coatings[26] are a versatile platform for the assembly of antimicrobial coatings on diverse substrates. Antimicrobial peptides, including nisin,[27] magainin Ⅱ,[28-29] synthetic antimicrobial peptide CWR11,[30] cecropin B,[31] SESB2V,[32] and antimicrobial lipopeptides[33] have been grafted to surfaces utilizing dopamine coatings. While such AMP conjugated coatings showed antibacterial efficiency, they were challenged by the poor performance against protein fouling and bacterial adhesion resulting in diminished antibiofilm activity over the long-term in vitro, and in relevant animal models. Inactivation of such antimicrobial technologies is driven by the accumulation of proteins and dead bacteria killed by contact killing on the surface providing a pedestal for subsequent biofilm formation by live bacteria. Therefore, coatings that resistant to protein and bacterial adhesion, and have antimicrobial moieties tethered to the surface, are more advantageous to combat implant/device-related infections.[34-35] Reches *et al* designed an AMP with three moieties (adhesive dopamine moiety, antimicrobial and antifouling motifs) and achieved dual functionality that resists biofouling.[36] Yang et al realized this function by conjugating both polylysine and copolymer with zwitterionic segments.[35] These studies demonstrate the potential of dopamine based substrate independent coatings for preventing infection on devices and implants.

Recently, we developed a simple, one-step, substrate independent antifouling coating utilizing self-assembly of polydopamine and hydrophilic polymers with very high molecular weights.[37-38] The antifouling efficiency of the coating was optimized by screening diverse hydrophilic polymers that can be self-assembled with polydopamine which resulted in the identification ultra-high molecular weight poly(*N,N*-dimethylacrylamide) as an anti-fouling agent. In this manuscript, we advanced this knowledge to create a dual functional coating. We reasoned that a coating that is easy to adapt, substrate-independent, functional and can generate excellent non-fouling surface could potentially be used as a method for screening surface tethered AMPs for antibiofilm activity in a relevant setting, and could thus be directly translated as implant and device coatings with greater chance of success. We initially investigated the conjugation of AMPs onto different non-fouling coatings and evaluated the influence of coating structure on antibiofilm activity. Subsequently, we used this platform and rapid assembly method to screen peptide conjugation and antimicrobial activity in a 96-well plate format to identify potent surface-tethered AMPs. The influence of AMP chemistry and their surface presentation on the antibiofilm activity on the coatings were investigated using a diverse repertoire of gram-positive and gram-negative bacteria *in vitro*. The success of the new screening method is demonstrated by the translation of bifunctional coating onto urinary catheters and testing of their antibiofilm activity *in vivo* using a clinically relevant mouse medical device infection model.

2. Materials and methods

2.1 Materials

Ultra-high molecular weight poly(*N*,*N*-dimethylacrylamide) (uhPDMA) was synthesized by atom transfer radical polymerization.[37] *N*-(3-Aminopropyl) methacrylamide hydrochloride (APMA) (98%) was purchased from Polysciences, USA and used without further purification.. All other reagents including 1, 1, 4, 7, 10, 10-hexamethyl triethylene tetramine (HMTETA) (97%), Tris[2-(dimethylamino)ethyl]amine (Me_6TREN) 97%, methyl 2- chloropropionate (97%), CuCl (99%), $CuCl_2$ (99%), 1-thioglycerol (97%) were purchased from Sigma-Aldrich (Oakville, ON). A single-side-polished silicon wafer (University Wafer, Boston, MA) deposited with titanium was prepared by e-beam evaporation of titanium following previously published protocols.[11]

SurFlash®I.V. Polyurethane catheter (Cat. #SR*FF1451, #SR*FF2419) were purchased from Terumo. Antimicrobial peptides, E6 (RRWRIVVIRVRRC-NH_2), Tet20C (KRWRIRVRVIRKC-NH_2), DJK5C (vqwrairvrvirc-NH_2) and 3002C (ILVRWIRWRIQWC-NH_2) with cysteine at the C-terminus (purity > 95%) were synthesized by Canpeptide Corp (Quebec, Canada). Peptide IDR-1018 (VRLIVAVRIWRR-NH_2) at >95% purity was purchased from CPC Scientific (Sunnyvale, CA). Tet20LC (KRWRIRVRVIRK-bA-bA-C-NH_2) was synthesized and purified (>90%) by the Hilpert laboratory by automated solid-phase peptide synthesis (SPPS) on a MultiPep RSI Peptide Synthesizer (INTAVIS, Tuebingen, Germany) using the 9-fluorenyl-methoxycarbonyl-tert-butyl (Fmoc/tBu) strategy.[39] Minimum inhibitory concentrations (MICs) of cationic peptides were measured using broth microdilution method with minor modifications.[40]

2.2 Synthesis of copolymer of N,N-dimethylacrylamide and N-(3-aminopropyl) methacrylamide (PDMA-co-APMA)

Copper (II) chloride (3 mg), copper (I) chloride (20 mg) and Me_6TREN (120 µL) were added successively into a glass tube. Milli-Q water (20 mL) was added, and the solution was degassed using three freeze-pump-thaw cycles. DMA (2 mL) and APMA (346 mg) was added into the glass tube and degassed with another freeze-pump-thaw cycle. The initiator (methyl 2-chloropropionate) methanol solution (20 µL from a stock solution of 80 µL in 10 mL methanol) was added successively to the reaction mixture, and the polymerization was kept at room temperature (RT) (22 °C) for 24 h. The polymerization solution was collected and purified by dialysis (molecular weight cut off: 1000 Da) against water (pH was adjusted to 8 by using 0.1M NaOH) for 3 days with daily exchange of water. The polymer was obtained by lyophilization the solution. The absolute molecular weight of PDMA-*co*-APMA was determined by gel permeation chromatography (GPC) following previously reported protocols.[11] ^{1}H NMR spectra were obtained on Bruker Avance NMR spectrometer (300 MHz) with using deuterated solvents. The solvent peak was used as a reference.

2.3 Synthesis of PDMA-co-APMA with iodoacetyl linker (PDMA-co-APMA-I)

The copolymer (PDMA-*co*-APMA, 100 mg) was dissolved in anhydrous acetonitrile (10 mL). Iodoacetic acid *N*-hydroxysuccinimide ester (70 mg) was added into the solution. The reaction was stirred overnight. The solution was dialyzed against water for 3 days with daily exchange of water. The solution was finally dialyzed against 5 mM Tris buffer (at pH 8.5) and concentrated to the solid content about 12 mg/mL as measured by Thermogravimetric Analysis (TGA Q500, TA Instruments, USA) and characterized by NMR.

2.4 Preparation of coating on the titanium, polyurethane catheters and 96 well plate surface

2.4.1 PU catheter

PU catheters with different sizes (14G and 24G) were initially cleaned by nitrogen plasma treatment and immediately coated using the previously published protocol.[38] The 24G catheter for *in vivo* study was coated twice by using the same solution composition.

2.4.1 Titanium substrate

The coating on the titanium substrate was prepared using the same protocol as that of PU catheter.

2.4.3 Microtiter 96-well plate

Microtiter 96-well plates were initially cleaned by nitrogen plasma treatment. The wells in 96-well plate were immediately coated with dopamine/uhPDMA mixed solution (250 µL, 2 mg/ml and 10 mg/ml respectively in 10 mM Tris buffer, pH 8.5). A second coating was applied using

200 μL solution having the same composition. The coated 96-well plate was then rinsed by Mill-Q water and dried under a stream of argon gas.

2.5 AMP *conjugation onto PDA/uhPDMA and PDA/PDMA-co-APMA-I coated surfaces*

The Ti surface or catheter coated with PDA/uhPDMA or PDA/PDMA-*co*-APMA-I was fully immersed into the peptide solution (0.6 mL, 0.1 mg/mL in 10 mM phosphate buffer (pH ~8) overnight followed by adding 1-thioglycerol (6 μL, at a final concentration of 10 μL/mL) for 24 h. For the 96 well-plate, 250 μL peptide solutions (0.1 mg/mL in 10 mM phosphate buffer, pH ~8) were added into the wells and incubated overnight followed by addition of 1-thioglycerol (2.5 μL, final concentration of 10 μL/mL) for 24 h. The peptide conjugated substrates were rinsed with milli-Q water thoroughly and dried under argon flow. The mass of peptides grafted onto the surface was calculated by the following equation $m = \rho \cdot h \cdot A$: where h represents the increase in thickness after peptide immobilization measured by ellipsometry; ρ is the volumetric mass density of antimicrobial peptide (1.5 mg/cm^3);[41] A is the surface area (cm^2).

2.6 Antibiofilm efficiency of AMPs assembled on Ti substrate

Pseudomonas aeruginosa (luminescence tagged strain PAO1 Tn7:P*lac-lux)*, and *S. saprophyticus* strain (ATCC 15305) were sub-cultured for testing the antibiofilm activity of the coating. An initial concentration 5 × 10^5 CFU/mL was used for these analyses. The coated Ti substrate along with the pristine Ti substrate were placed into a 24-well plate and was sterilized by immersing in 1 mL of 70% ethanol for 5 min. After the removal of ethanol, samples were each rinsed with 1 mL of sterile phosphate-buffered saline (PBS) for a total of 3 times. After the removal of PBS media from the last rinse, 1 mL of the prepared bacterial culture (~5 × 10^5 CFU/mL) of *S. saprophyticus* in Tryptic soy broth (TSB) or *P. aeruginosa* in Luria Broth (LB) was added to each sample. The 24-well plate was incubated at 37°C with shaking at 50 rpm for 6 h or 24 h. The samples were then thoroughly rinsed with PBS buffer, stained with green SYTO9 for all bacteria and red propidium iodide (PI) for dead bacteria. The stained bacteria on the Ti surface were examined by fluorescence microscopy (Zeiss Axioskop 2 plus, Thornwood, NY) and the antimicrobial activity of the surface was calculated using previously published method.[11] The samples that were incubated for 24 h also analyzed using C2+ confocal microscope (Nikon) with the 488 and 561 nm channels. All images were acquired using the same acquisition settings. The experiments were repeated 3 times, and representative results from an experiment are shown.

2.7 Antibiofilm efficiency of AMPs assembled on the catheter surface

Different sized catheters (14G and 24G PU), were cut into 1 cm sections and used for the study. The antibiofilm efficiency of AMPs immobilized catheter surface was measured using our previously published protocol.[38] The experiment has been repeated 3 times with similar results, and the representative results from one experiment are shown.

2.8 Screening and identification of surface conjugated AMPs with antibiofilm activity on a 96-well plate

Bioluminescence-tagged bacterial strains used in this study included *S. aureus* (Xen36), *P. aeruginosa* (PAO1.lux), *E. coli* (E38.lux), and *S. saprophyticus* (ATCC 15305). The antibiofilm activity of AMP conjugated coating on a 96-well plate was evaluated using our previously published protocol.[38] The experiment was repeated 3 times with 3 technical replicates per biological replicate.

2.9 Evaluation of antibiofilm efficiency of AMP coating on 24G PU catheters in a mouse urinary infection model

A total of 48 male C57BL/6 mice (Harlan®) at 10 weeks of age were included in experiments. Twenty mice were included in the control group (bare catheter) and 14 mice for each treated group (AMPs conjugated catheter, E6 and Tet20LC). The implantation of the catheter was performed following a procedure published previously our groups.[38],[42] One day after catheter implantation, all mice were anaesthetized and *S. saprophyticus* (1×10^7 CFU/mL in 50 µL PBS) was percutaneously injected into the bladder. At 7 days post-instillation of *S. saprophyticus,* all mice were sacrificed by CO_2 asphyxiation and the number of bacteria in the urine was quantified via serial dilutions and CFU counts. Indwelling catheters were collected, rinsed in 200 µL of sterile PBS three times and finally placed in 100 µL PBS. Seventeen from 20 explanted catheter samples in the control group and eleven from 14 for the coated group were sonicated for 10 minutes to aid biofilm dispersal. Samples were then vortexed at high speed for 10 sec, and bacterial numbers were determined by serial dilutions and CFU counts. Three catheters from each group were prepared for SEM (Hitachi SU3500) observation.[38]

There were 5 cases of unsuccessful infection with *S. saprophyticus* in the control group and 4 in the coated group of E6 and 2 in the coated group with Tet20LC as the CFU reading on both catheter surface and in urine was zero.

2.10 Cytocompatibility of BA and BA-E6 coated PU substrates

Three sample groups were included in the study, including bare PU substrate, BA and BA-E6 coated PU substrates (Diameter of 5/8"). The cytocompatibility of uncoated PU and coated PU substrates was measured using our previously established protocol.[38]

2.11 Hemolysis measurement of BA and BA-E6 coated PU substrates

Blood was collected from healthy donors at the Centre for Blood Research, University of British Columbia (the protocol for blood donations was approved by the University of British Columbia's clinical ethics board) into 3.8% sodium citrated vacutainers. The substrates were placed in the wells of 24-well culture plates containing 1 mL fresh collected whole blood. The plate was incubated at 37°C for 4 h with gentle shaking. The hemolysis was determined using the Drabkin's method.[43]

2.12 Surface characterization of AMP coating

ATR-FTIR spectra and water contact angle of the surfaces were measured using our previously published procedures.[12,38] X-ray photoelectron spectroscopy (XPS): Measurements were carried out at Nanofabrication and Characterization Facility (nanoFAB), University of Alberta. The spectra were collected using a Kratos Axis Ultra X-ray photoelectron spectrometer operated in energy spectrum mode at 210 W Spectra were fit using CasaXPS (VAMAS) software and were calibrated to the lowest binding energy component of the C1s emission at 284.6 eV. Two replicates per sample were analysed by XPS. Ellipsometry measurements: The thickness of the coating was measured by fitting the ellipsometry spectra with a multilayer Cauchy layer model[11]. QCM measurements: AMP conjugation on the surfaces was monitored in real-time by QCM-D (Q-sense AB, Sweden) at room temperature by tracking the changing in resonant frequency. The BA coating was initially deposited on SiO_2 (~50 nm) coated sensors and mounted into the QCM-D chamber. After stabilization of the baseline with buffer, a 0.1 mg/mL AMP E6 solution (pH 8.0) was flowed (50 µL/min) over the sensor. Finally, phosphate buffered saline (pH 8.0, 10 mM) was flowed to remove physically absorbed peptides. The mass was fitted through the Sauerbrey equation by using Qsense Dfind 1.2.2. Atomic force

microscopy analysis: Measurements were performed on a commercially available multimode system (Dimension 3100) with a maximum scan size of 130 μm ×130 μm, controlled by a NanoScope IIIa controller (Digital Instruments, Santa Barbara, CA). The surface morphology and adhesive force in PBS buffer was collected in the contact mode using V-shaped silicon probe (Bruker, NP-S10) with a spring constant ~0.06 N/m.

2.13 Statistical Analysis.

All the data values are presented as mean ± standard error (SE). Statistical significance was determined using a Student's t test, $p < 0.05$ was considered statistically significant.

3. Results

3.1 Influence of polymer coating structure on AMP conjugation and activity

3.1.1 Synthesis of coatings with different structure and their surface characterization

Figure 1 shows the structure of the constructed two AMP conjugated coatings. Experiments were performed using a Silicon wafer coated with Ti as a model surface for thorough characterization. AMPs with cysteine at the C-terminus was utilized for the conjugation into the coating. AMP E6 was used for initial investigation as it variant (without cysteine at the C-terminus) demonstrated strong broad-spectrum antimicrobial activity in soluble form.[44-45] E6 in tethered form also showed strong antibiofilm activity.[11-12]

In the first approach, we initially constructed a non-fouling surface coating using a rapid assembly of polydopamine (PDA) and ultra-high molecular weight PDMA (uhPDMA) (800 KDa, PDI 1.3) which is highly stable and can be prepared on any substrate.[37-38] The uhPDMA self-assembled with PDA nanoaggregates to generate surface coating layer where uhPDMA polymer chains non-covalently bound to the surface bonded PDA at multiple anchoring points to generate a thin coating. The coating was highly hydrophilic and enriched with uhPDMA chains on the surface. The coating was further modified with AMP E6. The conjugation (Figure 1A) utilized Michael-type addition reaction between the free -SH and -NH_2 groups on E6 and quinone functionality on PDA.[46] The uhPDMA chains were not modified as it did not have any reactive functionalities. The anticipated structure of the coating is that peptide E6 conjugated to the bottom PDA layer protected by the non-fouling PDMA chains emanating from the PDA anchor (see section 3.1.2 for more details). This approach is referred to as the BA-AMP coating throughout the manuscript since the AMP was attached only to the bottom layer of the coating.

In the second approach, a copolymer PDMA-*co*-APMA (*N*-(3-aminopropyl) methacrylamide) (Mn 630 000, PDI 1.3) was synthesized with APMA molar content of 10% (Supporting information, Figure S1). The amount of APMA component is restricted to 10 mol% to retain the non-fouling properties of the PDMA.[12,47-48] The copolymer was modified with iodoacetic acid (with a conversion of 60%, supporting information, Figure S2) to generate reactive groups for cysteine containing peptides on the polymer chains. This modified co-polymer was used for the generation of the non-fouling coating. PDMA-*co*-APMA-I was co-assembled with dopamine to generate a stable thin surface coating (Figure 1B) which was then conjugated with AMP E6. The chemistry of AMP conjugation is shown in Figure 1B. The peptide was conjugated both to the hydrophilic polymer component as well as on the PDA layer. Cysteine labeled E6 reacted with iodoacetamide groups on the PDMA-*co*-APMA-I copolymer chain as well as the quinone groups of PDA layer of the surface coating. This resulted in the generation of a structure where the AMP was distributed throughout the coating. This is referred to as the MA-AMP coating throughout the manuscript since the AMPs are attached at multiple sites throughout the coating.

The coating formation and peptide conjugation were initially investigated using ATR-FTIR analysis (Fig. 2A, B). The incorporation of uhPDMA and PDMA-*co*-APMA-I within the coating was evidenced by the shoulder peak at 1622 cm^{-1} due to the carbonyl group stretching (amide I band). The conjugation of AMP (E6) on the surface was demonstrated by the shoulder peak at 1634 cm^{-1} on BA-AMP and MA-AMP coatings after AMPs conjugation. The subtraction spectra, before and after peptide conjugation, highlights the prominent peak at 1634 cm^{-1} attributed to the C=O stretching for the amino acids in the AMPs, which confirmed the successful incorporation of AMPs in the coating. The incorporation of uhPDMA or APMA-*co*-APMA-I, and AMPs on the coating was further evidenced by the XPS analysis. The decrease in the silicon content for the coated substrate indicated the complete coverage of polymer coating on the substrate. The XPS survey scan (Fig. 2C) for the BA and BA-AMP coatings showed an increase in the nitrogen content in the coating compared to the PDA coating (Table 1). The presence of sulfur peak (S2p) (from cysteine residues) confirmed the presence of AMPs on the surface. In the case of the MA and MA-AMP coating, the presence of iodine(I3d) confirmed the successful incorporation of PDMA-*co*-APMA-I within the coating. The presence of S(2p) peak after AMPs (E6) conjugation, the disappearance of I(3d) peak in survey scan, and the change in elemental composition of the AMP immobilized surface (Table 1) confirmed the successful conjugation of E6 onto MA coating.

The conjugation of AMP to BA and MA coatings was further analyzed using water contact angle measurements. In comparison to the Ti substrate having a water contact angle of 68.5 ± 2º, the water contact angle of BA coating and BA-AMP coating were 31 ± 0.9º, 36.2 ± 0.4º respectively. In the case MA-AMP coating, the water contact angle was 37.9 ± 0.9º compared to 29.2 ± 1º for MA coating (Fig. 2D). Evidence for AMP conjugation was further obtained from the coating thickness measurements by ellipsometry. The dry thicknesses of BA and MA coatings were 17.2 ± 0.2 and 12.3 ± 0.5 nm, respectively. Upon conjugation of AMP E6 resulted in increases in thicknesses of 2.6 ± 0.2 nm and 2.8 ± 0.3 nm, respectively for the BA-AMP and MA-AMP coatings (Fig. 2E). The masses of grafted E6 on the BA and MA coating were 390 ± 30 ng/cm^2 and 420 ± 45 ng/cm^2 respectively. This calculation assumed that increase in thickness of the coating corresponded to the mass increase from the deposition of peptide E6.[48] The grafting of E6 onto the BA coating was further monitored in real-time using QCM-D to demonstrate the surface conjugation of the AMP (Fig.2F). The amount of AMP E6 bound to the BA surface increased sharply in the first 2 h and reached a plateau after 8 h. The amount of AMP E6 that remained on the surface was 568 ± 72 ng/cm^2 after rinsing with buffer. The grafting density measured by QCM-D was higher than that measured by ellipsometry as the mass measured by QCM-D includes a substantial amount of bound water, whereas ellipsometry measured the conjugated AMP E6 mass in the dry state, and is consistent with previous work on mass quantification by QCM-D.[49] The coatings were further characterized for stability in buffer solutions; there was no noticeable change in thickness observed after immersing the BA-AMP coating in PBS buffer for 7 days at 37°C, or underwent ultrasonication for 10 min in water.

3.1.2 Evidences for differences in structure of polymer chains and presentation of AMPs within the coating by AFM analysis

To gather the information on surface structure of two different coatings (BA-AMP and MA-AMP), we utilized AFM analysis in wet conditions. Figure 3A and B shows the surface morphology of BA and BA-AMP coating on Silicon substrate. The BA coating is relatively smooth as the low surface roughness (0.5 nm) is comparable to bare substrate (0.2 nm, Figure S3, Supporting Information). The surface roughness increased to 0.8 nm after conjugating AMP (BA-AMP (E6)). AFM force studies were used to probe the coatings. The representative force curves for BA and

BA-AMP coatings are shown in Figure 3. The typical force profile for steric repulsion exerted by polymer chains in AFM approach curve is reminiscent of a swollen brush layer grafted onto the surface for BA-AMP (E6) coating (Fig. 3C). The AFM retraction curve for BA-AMP coating gave a characteristic profile of stronger adhesive force at shorter distances compared to the BA coating before AMP conjugation. Figure 3D, E show the probability distribution histograms of maximum adhesive force and rupture distance for BA-AMP (E6). The stronger force (1.1 ± 0.1 nN) at shorter rupture distance (58.6 ± 7.5 nm) could be due to the interaction between the peptide conjugated to the underlying PDA, and the hydrophobic AFM tip. This argument is supported by the fact that the retraction force curve for PDA-E6 coating (without the non-fouling uhPDMA chains) also showed similar characteristics in the probability distribution histograms with maximum adhesive force (2.2 ± 0.2 nN) and rupture distance (47.4 ± 5.3 nm) (Figure S4, Supporting Information). The smaller adhesive force (0.26 ± 0.04 nN) at longer distance (306 ± 100 nm) indicated the rupture of the adhered uhPDMA chains from the AFM tip. This data suggests that the PDMA chains on the surface might be adopting a looplike assembly.[37] The data clearly showed that a swollen brush like structure due to the presence of uhPDMA chains was not completely lost and the chains offer steric protection even after AMP E6 conjugation. Together these data indicate that E6 was conjugated to the coating which was protected by the swollen uhPDMA layer.

Figure 4A and B shows the surface morphology of MA and MA-AMP coating. Upon conjugation of AMP, the surface roughness of MA coating increased from 0.3 nm to 0.5 nm for MA-AMP (E6) coating. The representative AFM force curves for the MA and MA-AMP (E6) coatings are shown in Figure 4. There is a weak jump-to-contact (JTC) force in the AFM force profile for both MA and MA-AMP coatings. The data suggest that the copolymer modification resulted in a different surface assembly compared to BA and BA-AMP coatings.[12,48] During retraction, or pull-off, a stronger adhesive force 0.8 ± 0.1 nN was observed in the case of the MA coating which increased to 2.6 ± 0.2 nN when AMP E6 was conjugated. The strong adhesive force was due to the hydrophobic interaction between the AFM tip and the surface. The data indicated that in the case of the MA-AMP E6 coating, the more hydrophobic AMP E6 is presented on the outer layer without much steric protection from the copolymer resulting in strong hydrophobic interaction with the AFM tip. The probability distribution histograms of maximum adhesive force and rupture distance are shown in Fig. 4D, E for MA and MA-AMP (E6), respectively. The weak jump-to-contact (JTC) force observed in the approach curve also indicated that the steric protection by the polymer chains in this structure might be low.[12,48] All these results pointed to a different structure of PDMA-*co*-APMA-I chains in the MA coating compared to PDMA chains in BA coating. There was no rupture observed at long distance, which suggests that the polymer chains were more confined onto the PDA layer and had less freedom to stretch out. Taken together, these data indicate that AMP E6 was present throughout the coating layer in the MA-AMP coating compared to the BA-AMP coating. The shielding ability of the non-fouling PDMA component was also relatively weak in the case of the MA-AMP coating.

The data clearly show that the structure of polymer chains and the presentation of AMPs (E6) were quite different for both BA-AMP and MA-AMP coatings. This allowed us to further investigate the role of presentation of AMP and coating structure to their antibiofilm activity.

3.1.3 Antibiofilm efficacy of AMP E6 conjugated BA-AMP and MA-AMP coatings

We further evaluated the influence of AMP presentation and coating structure on the antibiofilm activity. A live/dead assay was employed to examine both the level of bacterial adhesion and the viability of adhered bacteria in early-stage biofilm formation. Figure 5 shows the number of adhered *S. saprophyticus* on different coatings after incubating with bacteria for 6h and 24h, as

well as the proportion of dead bacteria. The BA-AMP (E6) was more resistant to bacterial adhesion when compared to the BA binary coating; the bacterial densities at 6 h were 57 ± 12 and 29 ± 15/mm^2 for the BA and BA-AMP coatings respectively. The MA coating showed similar activity in reducing bacterial adhesion compared to the BA coating; there were comparable numbers of adherent bacteria (66 ± 15/mm^2). In contrast, the MA-AMP surface had more bacteria adhered onto the surface (167 ± 17/mm^2). The percentages of dead bacteria were 6.3%, 18.2%, 8.2% and 18.3% for the BA, BA-AMP, MA, and MA-AMP coating respectively (Fig. 6C). The MA coating did not show the antibacterial activity. The low molar percentage of APMA (10 mol%) and the conversion of amine groups in the APMA segment to amide groups by iodoacetic acid decreased the primary amine content on the coating resulting in the poor activity observed. The increased percentage of dead bacteria on BA-AMP and MA-AMP demonstrated moderate early killing efficiency of AMPs conjugated to the non-fouling coating system.

Next, we studied potential changes in membrane integrity and morphology upon interaction of the bacteria with the surface tethered AMPs on the coating using scanning electron microscopy (SEM). The bacteria on the control and BA coated substrates were observed to have a smooth surface (Fig. 5F,G), while those on BA-AMP and MA-AMP surfaces showed membrane collapse (Fig. 5H,I) and compromise of membrane integrity. This indicates that the surface-tethered AMPs generated using our coating interact with and kill bacteria via electrostatic disruption of the membrane, a mechanism that has been previously described.[11,50-51]

We further evaluated the early-stage biofilm formation at 24 h. Figure 5 and Figure 6A show the fluorescence and confocal images of bacteria adhesion on bare and coated substrates. Figure 5A and 6A showed that biofilm developed on the bare substrate. There was a great reduction in biofilm formation on the BA and BA-AMP coated surfaces. Only a few bacterial colonies were observed on the BA-AMP coating (Fig. 6C) confirming the strong inhibition of biofilm formation. The BA and BA-AMP surfaces had similar numbers of adhered bacteria compared to 6 h (52 ± 7/mm^2, 25 ± 9/mm^2, respectively). In contrast, the MA and MA-AMP showed an increase (82 ± 34/mm^2 and 191 ± 51/mm^2) in the number of adhered bacteria compared to 6h. The AMP conjugated surfaces (BA-AMP and MA-AMP) sustained their antimicrobial activity as similar percentages of dead bacteria (14.8% and 19.7%) were recorded.

A similar observation was made for *P. aeruginosa* (Fig. 6). The BA-AMP (E6) coating showed greater efficiency in preventing bacterial colony formation on the surface. The activity was higher for the BA-AMP (E6) coating compared to MA-AMP (E6) suggesting that the presentation of AMP and coating structure influenced the antibiofilm activity.

3.1.4 Antibiofilm efficacy of BA-AMP (E6) and MA-AMP (E6) coating on polyurethane surface

We further analyzed the efficiency of the coating to prevent biofilm formation on a biomedical plastic surface relevant to catheter-associated urinary tract infections. We adapted the coating methodology on the surface of 14G PU catheters. The pristine catheter, BA, BA-AMP, MA and MA-AMP coating on PU catheters were tested by assessing the number of adhered bacteria on the surface by assessing CFUs after 24 h of incubation. Figure 7 shows the adhesion of *S. saprophyticus* (A) and *P. aeruginosa* (B) on differently coated surfaces. The BA coating alone was able to reduce the adhesion of gram-positive *S. saprophyticus* by about 87.9% compared to the uncoated catheter which was consistent with previous reports.[38] Upon conjugation of E6 (BA-AMP), the antibiofilm activity of the coating increased to 98.4% ($p < 0.05$). However, MA-AMP (E6) could not reduce the biofilm formation in comparison to the control coating without peptides or BA-AMP coatings. Similar results were observed for the gram-negative bacteria, *P. aeruginosa.*

From these results of bacterial adhesion and early-stage biofilm formation, it was determined that presentation of AMPs on the coating and the coating structure had a significant influence on their antibiofilm activity. The BA-AMP coating, where the AMP is conjugated on the PDA layer and protected by the non-fouling uhPDMA chains showed significantly higher activity than the coating where AMPs were presented throughout the coating (MA-AMP). Since the synthesis method for BA-AMP coating is simple, we anticipate that this method could be easily and rapidly adapted to diverse surfaces and diverse peptides rapidly, both as a screening method for surface specific peptides in an antifouling background as well as an infection resistant coating.

3.2 Development of a screening and identification method for potent surface immobilized antibiofilm peptides in a relevant antifouling background

To develop a robust screening protocol in a realistic environment which could be potentially used to test implant and device modifications, we initially tested a small library of AMPs peptides (Table 2) with broad-spectrum activity. Besides E6, Tet20C and its variant Tet20LC, IDR-1018, 3002, and D-enantiomeric peptide DJK5 and its variant, were also included in the study. Tet20C (KRWRIRVRVIRKC) and Tet20LC (KRWRIRVRVIRK-bA-bA-C-$CONH_2$) are variants of AMP Opt5 (KRWRIRVRVIRK-$CONH_2$), which showed high antimicrobial activity in soluble and tethered form against various pathogens.[23,52] Adding a cysteine at C-terminus of Opt5 resulted in Tet20C. Tet20LC has a linker consisting of two beta-alanine added before the cysteine. Tet20C showed strong antibiofilm activity while tethered in the brush coating on surface.[49,51] Peptide IDR-1018 was developed based on bactenecin and possessed both immunomodulatory activity and antibiofilm activity.[53] Peptide 3002 as a variant of IDR-1018, was discovered with computer aiding and exhibited stronger antibiofilm activity than IDR-1018.[54] DJK5 and its variants was recently developed D-enantiomeric protease-resistant peptide with a more potent activity in inhibiting biofilm formation relative to L-amino acid IDR‐1018.[55] This proven initial library of peptides (Table 2) was used to test our concept on the application of BA-AMP coating as a screening tool to identify optimal surface tethered peptide that prevents biofilm formation in an antifouling background.

Initial studies were performed using a silicon wafer coated with titanium and the data showed that different AMPs could be successfully conjugated onto the BA coating (Figure 8B). Based on this, we adapted the coating technique to a 96-well plate made of polypropylene (pp) for a medium-throughput screening of surface conjugated AMPs against diverse bacteria (Figure 8A). We measured the bacterial adhesion on the BA coating and uncoated pp wells when compared to AMP conjugated wells. An antibiofilm assay based on bioluminescence readout was developed to evaluate the efficiency of the coating and for identifying peptides with the best activity against biofilm formation. Figure 8C shows the reduction of *S. saprophyticus* adhesion on different AMPs tethered on the BA coating upon incubation with bacteria over 24 h. The bioluminescence readout was confirmed with CFU counts in the case of the BA-AMP (E6) coating (Fig. 7). AMPs Tet20C, Tet20LC and DJK5C (containing as added cysteine at the C-terminus) showed almost complete reduction of biofilm formation (~100%; $p = 0.002$, $p = 0.01$, $p = 0.003$ respectively, pp vs BA-AMP). In contrast, AMPs DJK5, DJK6, IDR-1018 and 3002 showed no significant improvement over the BA coating (83.4%, $p = 0.98$, 83.5%, $p = 0.97$; 82.2%, $p = 0.71$ and 81.7%, $p = 0.84$ respectively). The peptide conjugated coating was also tested against *S. aureus* (Fig. 8D). Tethering E6 into the coating further reduced the biofilm formation (93%) compared to the BA coating (90.7%) ($p = 0.54$, BA vs BA-E6). Near complete reduction was seen on the, Tet20C, Tet20LC conjugated surface (98.8%, $p = 0.003$; and 100% $p = 0.002$, pp vs BA-AMP). Surface conjugated with DJK5C, DJK5, IDR-1018, 3002C showed similar reduction levels compared to tethered E6 (95.1%, $p = 0.004$; 90.5%, $p = 0.004$; 93.5%,

p = 0.004; 93.6%, p = 0.004; pp vs BA-AMP). We also investigated the activity against *P. aeruginosa*, which showed that tethering E6, Tet20C, Tet20LC and DJK5C resulted in the largest reduction of biofilm formation (98.2%, p = 0.0002, 99.6%, p = 0.0002, 100%, p = 0.0002, and 99.1%, p = 0.0002, respectively, pp vs BA-AMP) (Fig. 8E). DJK6, RI-DJK5, 1008 and 3002C have less biofilm reduction compared to BA coating (58.8%, 76.2%, 83.2% and 32.4%, respectively). Peptide conjugation also helped to provide additional reduction in *E. coli* biofilm formation (91.8% for tethered E6, p = 0.008, pp vs BA-E6) (Fig. 8F). There was no significant difference in reduction efficiency observed for *E. coli* between the different peptides.

Overall, the 96-well-based antibiofilm screening assay developed by conjugation of AMPs to a non-fouling background helped us to identify AMPs with better antibiofilm activity. We determined that peptides, E6, Tet20C, Tet20LC and DJK5C showed better broad-spectrum activity than the other tested peptides from the library against the most common uropathogens.

3.3 Biocompatibility of BA-AMP coating

Hemolysis analysis was performed to determine the hemolytic properties of the AMP conjugated coating when in direct contact with blood. The result of the hemolysis analysis showed that the BA and BA-E6 coating causes very low hemolysis, 0.4% and 0.3%, respectively (Fig. 9A). The data suggest that the surface conjugated peptide is not hemolytic. To analyze cytocompatibility, a cell viability assay utilizing human bladder epithelial cells (T24) was performed.

The viability of adhered cells on the PU substrate coated with BA and BA-AMP was over 90% and was similar for both coated and uncoated substrates (Fig. 9B). These results suggest that BA-AMP coating has high biocompatibility.

3.4 Investigation of antibiofilm activity of lead AMPs tethered coatings in a mouse urinary infection model

We next investigated whether our new coating chemistry and data from the screening studies could be utilized for the prevention of implant/device infection. We adapted the coating chemistry to 24G catheters using two different peptides that showed greater promise (BA-E6) and BA-Tet20LC). The generated coatings on catheters were studied for their *in vitro* activity first before testing in mouse infection models (Figure 10A). The BA-E6 and BA-Tet20LC showed activity in preventing biofilm formation by 97.5% and 98.1%, respectively, compared to the 85% reduction seen on the control BA coating without peptides.

The efficiency in reducing biofilm formation was assessed using an ultrasound-guided percutaneous model of catheter-associated urinary tract infections.[42] The average CFU counts of bacteria in urine for mice bearing untreated control catheters was (3 ± 0.7) x 10^7 CFU/mL. For those implanted with catheters bearing BA-AMP (E6) and BA-AMP (Tet20LC) coatings, the CFU counts were (2.1 ± 0.7) x 10^7 and (1.8 ± 0.9) x 10^7 CFU/mL respectively, indicating that catheters from different groups were exposed to similarly infectious conditions (Fig. 10C). After 7 days post-instillation, the number of adhered bacteria on control catheters was (8.5 ± 2.4) x 10^4 CFU/catheter, whereas that for catheters coated with BA-E6 and BA-Tet20LC, was (3.4 ± 1.1) x 10^3 CFU/catheter, (2.5 ± 0.8) x 10^3 CFU/catheter, demonstrating a 96% and 97% reduction in bacterial adhesion respectively, when compared to the control (Fig. 10B).

The biofilm formation on the catheter surface was also examined by scanning electron microscopy (SEM). Figure 10 D, E, F shows the biofilm formation on the bare catheter and coated BA-AMP(E6) and BA-AMP (Tet20LC) catheters after 7 days post instillation. There was distinct biofilm formation on the bare catheter. The biofilm distributed along the catheter surface

rather than covering the whole catheter piece (Fig. 10D, Supporting Information, Figure S5). We found a layer of extracellular matrix deposited on the bare catheter surface (Supporting information, Figure S5). Biofilm was rarely seen on BA-E6 and BA-Tet20LC coated catheter (Fig. 10E, F). A non-continuous layer of extracellular matrix was observed on coated catheter surfaces (Supporting Information, Figure S5).

4. Discussion

Applying AMP-based coatings on medical devices/implants provides a promising approach to prevent medical device associated infections. There is extensive research into the development of new AMPs and their conjugation to the surface of medical devices.[19-36] The conjugation chemistry and the distribution, and presentation of AMPs on the coating were shown to influence the mobility and orientation of the conjugated peptides, resulting in the reduction of their bactericidal activity compared to the soluble forms.[56-58] The current approaches require multiple modification steps and need different chemical reactions to anchor peptides with different motifs, polymer and polymer-AMP coatings on diverse biomedical material surfaces. The development of simple and universal approaches would expand the application AMP based coatings on diverse medical devices irrespective of their shape, dimensions or their chemical nature. Polydopamine-based coatings showed good promise in this aspect as it is a substrate independent coating approach, however, non-specific interaction of bacteria and fouling agents with PDA based surface coating with AMP is challenging.

The use of a non-fouling matrix to integrate AMPs on the surface confers anti-adhesive properties.[12,47] This is an important consideration since the positively charged AMPs are known to promote protein adsorption as well as adhesion of dead bacteria or bacterial debris onto the coated surface leading to the passivation of the surface and loss of bactericidal activity.[34-36,59] Thus, a combination of anti-adhesive components and AMPs are necessary, and provide a promising approach to combat biofilm formation.[10,58] The contact killing by the AMP, and repulsion or release of live/dead bacteria from the surface by the non-fouling component play crucial roles in preventing biofilm formation. Thus, it is essential to optimize both bactericidal and antifouling properties to achieve better antibiofilm activity in complex environments such as *in vivo* conditions. Although, the importance of antifouling background is illustrated in multiple studies, the current screening protocols and identification of potent surface tethered AMPs did not take this aspect into consideration. Thus, the generation of a simple universal antifouling coating approach which has the ability to perform as a screening platform for new AMP identification with potent surface activity and can also easily translated as a biomedical device coating will have significant potential. We demonstrated both of these aspects in the present work to expand the potential of AMP based antibiofilm coatings.

Building on a substrate independent coating approach, we initially investigated the role of AMP's presentation on an antifouling background by generating sets of coatings with two different polymer structures on the surface. Our surface analyses including ATR-FTIR, contact angle measurements and AFM force measurements conclusively illustrated the differences in the presentation of AMPs on these coatings. Our studies demonstrated that direct conjugation of AMPs to the non-fouling polymer (MA-AMP coating) was not as effective in comparison to the situation where the peptide was presented within the antifouling layer without direct attachment to the polymer chains (BA-AMP coating). Although, the control non-fouling background in both cases (BA and MA coatings) without AMPs performed similar, potent long-term biofilm activity was only achieved when the AMPs are sterically protected. This data illustrated the importance of the characteristics of the antifouling layer and coating structure for the first time.

The importance of appropriate antifouling background in the antibiofilm performance for AMP coating is illustrated by the incorporation of the non-fouling component PDMA. In the absence of uhPDMA or its copolymer, the surface conjugated E6 accumulated more bacteria on the surface (Supporting information, Fig. S6). This demonstrates the advantage of the current coating approach over previously reported single functional PDA-AMP coatings.[27-33] The importance of polymer structure and the way in which AMPs are conjugated on the surface enable the long-term potent antibiofilm activity as illustrated using BA-AMP and MA-AMP coatings. The BA-AMP coating structure offered optimal protection of AMPs against non-specific adhesion of dead/live bacteria and retained the bactericidal activity by an electrostatic membrane disruption mechanism. The PDMA chains in the moderate brush regime were responsible for the antifouling characteristics of the BA-AMP coating and was helpful in preventing the deposition of bacterial debris on the surface avoiding surface passivation and retention of AMP activity, and thus providing a "regenerating" surface to kill bacteria.[60-64]

The increased bacterial adhesion shown by the MA-AMP coating could be due to the more accessible interaction of the cationic AMPs with negatively charged bacteria unlike BA-AMP coatings. Another reason might be the slightly higher hydrophobic character of the MA-AMP coating as revealed by the AFM force measurements. Unlike the BA-AMP coating structure, in the MA-BMP coating, the non-fouling properties of the hydrophilic PDMA were insufficiently protecting the surface. Overall, having active AMPs present on the coating at high density didn't outweigh the disadvantages of increased bacterial adhesion which contributed to the poor long lasting antibiofilm activity. Although the current data is illustrated in the case of AMPs, the same principle is highly relevant in the design criteria of bifunctional antibiofilm surfaces which utilize contact killing for its antibiofilm activity.

Another important consideration was the AMP candidate which works in cooperation with the non-fouling background. The secondary structure of the conjugated peptides could be altered upon interaction with the coating components[11,51] and could affect bactericidal activity of the AMP conjugated surface. Thus, it is important to evaluate and identify AMPs that work under relevant conditions. Compared to other AMP conjugation methods involving multi-step modification and substrate dependent chemistry,[15-19,35-36] the conjugation of AMP to the BA coating was highly efficient, substrate independent, and can be performed via a simple incubation without the need of any further modification. Thus, the developed method could be used as a high throughput screening method for developing novel AMPs with high surface activity in combination with the non-fouling background. Since PDA/PDMA coating is highly biocompatible,[65-66] it can be also readily translated to medical devices.

To illustrate the point and as a proof-of-concept, we conjugated a small library of AMPs to the BA coating and assessed their antibiofilm formation efficiency against both gram-positive and gram-negative bacteria. We explored the potential of the screening approach to identify potent surface immobilized peptides from a library of AMPs with excellent activity in soluble form (Table 2). The results from the antibiofilm assay confirmed the increased reduction in biofilm formation for the identified AMPs after conjugation. Importantly, the tethered peptides showed differences in efficiency in preventing biofilm formation when attached to the non-fouling background. The tethered AMPs (with cysteine at the C-terminus) have potent antibiofilm activity against *S. saprophyticus and E. coli*, consistent with their strong antimicrobial activity of their soluble form (Table 2). Tethered Tet20LC showed the best antibiofilm activity against *S. aureus,* even though it has the same MIC values as Tet20C. The addition of two beta-alanines with linear structure (Tet20C to Tet20LC), may have enhanced the flexibility of tethered peptides or the secondary structure[22,67] to maximize the interaction between tethered peptides

and bacteria. The tethered IDR-1018 and 3002C showed compromised antibiofilm activity against *P. aeruginosa* compared to other tethered peptides, which agrees with their weak antimicrobial activity in soluble form. In general, AMPs E6, Tet20C, Tet20LC and DJK5C showed better broad-spectrum activity against different pathogens compared to DJK5, DJK6, IDR-1018 and 3002C.

Another interesting observation was regarding the functional group used for covalent immobilization of AMPs. Covalent immobilization of DJK5 with or without cysteine at the C-terminus resulted in different activity profiles depending on the exposed peptide terminus. Tethered DJK5C in the coating showed better prevention of biofilm formation than N-terminal tethered DJK5 for all four bacterial strains tested. These results indicate that the covalent immobilization of its C-terminus (for DJK5C) allowed the peptides to have its *N*-terminal hydrophobic domain and full complement of amines interacting with bacteria to achieve higher bactericidal activity. This is consistent with the fact that peptide orientation is crucial to generate optimal interaction between the peptide "killing components" and bacteria to achieve high activity.[23,52] The hydrophobic domain and amines should be free to interact with the bacterial surfaces.

Further, we demonstrated the application of the developed screening and identification method for potent surface tethered antibiofilm AMP and the application of the coating chemistry to a medical application which is highly relevant in preventing catheter associated urinary tract infection. We directly applied the coating to polymeric catheters without changing the composition and illustrated its activity in a clinically relevant *in vivo* catheter-associated urinary tract infection model. This proof-of-concept study with identified peptides from a small library clearly demonstrates the potential of our developed screening approach for the identification of better peptides with improved activity for future studies. In addition, adaptation of this coating approach using other forms of peptide screening may prove useful in the prevention of implant/device-associated infections in other settings. This novel anti-adhesive coating consisted of a combination antimicrobial peptide E6 and Tet20LC tethered to an antifouling coating and demonstrated high efficiency in significant reducing biofilm formation on clinically used polyurethane catheter surface over a 7-day period. The enhanced prevention of biofilm formation in both *in vitro* and *in vivo* studies described here illustrates the versatility of the new coating method. While this AMPs conjugated non-adhesive coating showed excellent efficiency in reducing biofilm formation and infection, the use of different bacterial species and animal models by other studies investigating the efficacy of different coating technologies throughout the literature,[15-20,27-36] does not allow us to draw conclusions regarding superiority of our coating. For this, a direct comparison using similar conditions is needed. Importantly, unlike previously developed coatings, the current coating approach is simple, and versatile, and can be applied to diverse materials used in medical device manufacturing, making its translation potential into clinical practice high.

5. Conclusions

In summary, we have developed a new coating strategy which is simple and easily translatable onto diverse substrates for tethering AMPs onto a non-fouling background. The approach allowed for the presentation of AMPs at different locations within the coatings. The structure of the coating changed the distribution of AMPs within the coating, interaction of AMPs with bacteria, and both of these factors influenced their efficiency against biofilm formation. The coating with the non-fouling PDMA chains presented in the appropriate structure and provide steric protection to the surface immobilized AMPs showed the highest antibiofilm activity. The surface tethered AMPs and PDMA chains worked in cooperation to kill the bacteria on the

surface, minimized the bacterial adhesion, and regenerated the surface activity by preventing the accumulation and passivation by fouling agents. The optimized coating was adapted as a method for medium-throughput screening for the identification of surface tethered peptides with high antibiofilm activity on surfaces. Using this method, we identified a set of potent surface immobilized AMPs from a small library of peptides and were used to generate new antibiofilm coatings that works in complex environments. The new antibiofilm coating has shown to be highly effective in preventing biofilm formation *in vitro* and in a mouse infection model of medical device infection demonstrating the potential of the new coating method. The current study provided the design criteria for bifunctional coatings, and demonstrated that fine tuning of coating components is critical to achieve high antibiofilm activity on medical device/implants that works in relevant conditions.

Acknowledgements

This research was funded by the Canadian Institutes of Health Research (CIHR), Natural Science and Engineering Research Council (NSERC) of Canada, CIHR grant FDN-154287 to REWH and Michael Smith Foundation of Health Research (MSFHR). The authors thank the LMB Macromolecular Hub supported by Canada Foundation for Innovation (CFI) and the British Columbia Knowledge Development Fund (BCKDF). REWH is a Canada Research Chair in new anti-infective drug discovery and a UBC Killam professorship. DK is the recipient of a New Investigator award from CIHR. JNK is the recipient of a Career Investigator Scholar award from MSFHR.

Supporting Information Available: ^{1}HNMR spectra of synthesized copolymer PDMA-*co*-APMA and PDMA-*co*-APMA-I. Surface morphology and AFM force spectroscopy of Silicon wafer. AFM force spectroscopy of polydopamine conjugated with E6 peptide. SEM images of biofilm of *S. saprophyticus* on bare catheter and coated catheters. Bacteria adhesion on PDA and PDA-E6 coated Ti substrate. Biofilm growth condition for different bacteria.

References

1. Darouiche, R. O. Current concepts - Treatment of Infections Associated with Surgical Implants. *N. Engl. J. Med.* **2004,** *350*, 1422-1429.
2. Bryers, J. D. Medical Biofilms. *Biotechnol. Bioeng.* **2008,** *100*, 1-18.
3. Kostakioti, M.; Hadjifrangiskou, M.; Hultgren, S. J. Bacterial Biofilms: Development, Dispersal, and Therapeutic Strategies in the Dawn of the Postantibiotic Era. *Cold Spring Harb. Perspect. Med.* **2013,** *3*, article No. a010306.
4. Wolcott, R. D.; Rhoads, D. D.; Bennett, M. E.; Wolcott, B. M.; Gogokhia, L.; Costerton, J. W.; Dowd, S. E. Chronic Wounds and the Medical Biofilm Paradigm. *J. Wound Care* **2010,** *19*, 45-53.
5. Sui, Y.; Gao, X. L.; Wang, Z. N.; Gao, C. J. Antifouling and Antibacterial Improvement of Surface-Functionalized Poly(vinylidene fluoride) Membrane Prepared via Dihydroxyphenylalanine-Initiated Atom Transfer Radical Graft Polymerizations. *J. Membr. Sci.* **2012,** *394*, 107-119.
6. Ho, C. H.; Tobis, J.; Sprich, C.; Thomann, R.; Tiller, J. C. Nanoseparated Polymeric Networks with Multiple Antimicrobial Properties. *Adv. Mater.* **2004,** *16*, 957-961.

7. He, W.; Zhang, Y.; Li, J. H.; Gao, Y. L.; Luo, F.; Tan, H.; Wang, K. J.; Fu, Q. A Novel Surface Structure Consisting of Contact-active Antibacterial Upper-layer and Antifouling Sub-layer Derived from Gemini Quaternary Ammonium Salt Polyurethanes. *Sci. Rep.* **2016,** *6*, 32140.
8. Zhang, X. Y.; Zhao, Y. Q.; Zhang, Y. D.; Wang, A. Z.; Ding, X. K.; Li, Y.; Duan, S.; Ding, X. J.; Xu, F. J. Antimicrobial Peptide-Conjugated Hierarchical Antifouling Polymer Brushes for Functionalized Catheter Surfaces. *Biomacromolecules* **2019,** *20*, 4171-4179.
9. He, Y. Y.; Wan, X. Y.; Xiao, K. C.; Lin, W. W.; Li, J. H.; Li, Z.; Luo, F.; Tan, H.; Li, J. S.; Fu, Q. Anti-biofilm Surfaces from Mixed Dopamine-modified Polymer Brushes: Synergistic Role of Cationic and Zwitterionic Chains to Resist Staphyloccocus aureus. *Biomater. Sci.* **2019,** *7*, 5369-5382.
10. Gevrek, T. N.; Yu, K.; Kizhakkedathu, J. N.; Sanyal, A. Thiol-Reactive Polymers for Titanium Interfaces: Fabrication of Antimicrobial Coatings. *ACS Appl. Polym. Mater.* **2019,** *1*, 1308-1316.
11. Yu, K.; Lo, J. C. Y.; Mei, Y.; Haney, E. F.; Siren, E.; Kalathottukaren, M. T.; Hancock, R. E. W.; Lange, D.; Kizhakkedathu, J. N. Toward Infection-Resistant Surfaces: Achieving High Antimicrobial Peptide Potency by Modulating the Functionality of Polymer Brush and Peptide. *ACS Appl. Mater. Interfaces* **2015,** *7*, 28591-28605.
12. Yu, K.; Lo, J. C. Y.; Yan, M.; Yang, X. Q.; Brooks, D. E.; Hancock, R. E. W.; Lange, D.; Kizhakkedathu, J. N. Anti-adhesive Antimicrobial Peptide Coating Prevents Catheter Associated Infection in a Mouse Urinary Infection Model. *Biomaterials* **2017,** *116*, 69-81.
13. Xue, Q.; Liu, X. B.; Lao, Y. H.; Wu, L. P.; Wang, D.; Zuo, Z. Q.; Chen, J. Y.; Hou, J.; Bei, Y. Y.; Wu, X. F.; Leong, K. W.; Xiang, H.; Han, J. Anti-Infective Biomaterials with Surface-Decorated Tachyplesin I. *Biomaterials* **2018,** *178*, 351-362.
14. Chen, R. X.; Willcox, M. D. P.; Ho, K. K. K.; Smyth, D.; Kumar, N. Antimicrobial Peptide Melimine Coating for Titanium and its in vivo Antibacterial Activity in Rodent Subcutaneous Infection Models. *Biomaterials* **2016,** *85*, 142-151.
15. Salwiczek, M.; Qu, Y.; Gardiner, J.; Strugnell, R. A.; Lithgow, T.; McLean, K. M.; Thissen, H. Emerging Rules for Effective Antimicrobial Coatings. *Trends Biotechnol.* **2014,** *32*, 82-90.
16. Ahmadabadi, H.Y.; Yu, K.; Kizhakkedathu J. N. Surface Modification Approaches for Prevention of Implant Associated Infections. *Colloid Surf. B-Biointerfaces* **2020**, *193,* article No. 111116.
17. Godoy-Gallardo, M.; Mas-Moruno, C.; Yu, K.; Manero, J. M.; Gil, F. J.; Kizhakkedathu, J. N.; Rodriguez, D. Antibacterial Properties of hLf1-11 Peptide onto Titanium Surfaces: A Comparison Study Between Silanization and Surface Initiated Polymerization. *Biomacromolecules* **2015,** *16*, 483-496.
18. Mishra, B.; Basu, A.; Chua, R. R. Y.; Saravanan, R.; Tambyah, P. A.; Ho, B.; Chang, M. W.; Leong, S. S. J. Site Specific Immobilization of a Potent Antimicrobial Peptide onto Silicone Catheters: Evaluation against Urinary Tract Infection Pathogens. *J. Mat. Chem. B* **2014,** *2*, 1706-1716.
19. Sakala, G. P.; Reches, M. Peptide-Based Approaches to Fight Biofouling. *Adv. Mater. Interfaces* **2018,** *5*, article No. 1800073.
20. Riool, M.; de Breij, A.; Drijfhout, J. W.; Nibbering, P. H.; Zaat, S. A. J. Antimicrobial Peptides in Biomedical Device Manufacturing. *Front. Chem.* **2017,** *5*, article No. 63.

21. Falciani, C.; Lozzi, L.; Pini, A.; Bracci, L. Bioactive Peptides from Libraries. *Chem. Biol.* **2005,** *12*, 417-426.
22. Lopez-Perez, P. M.; Grimsey, E.; Bourne, L.; Mikut, R.; Hilpert, K. Screening and Optimizing Antimicrobial Peptides by Using SPOT-Synthesis. *Front. Chem.* **2017,** *5*, article No. 25.
23. Hilpert, K.; Elliott, M.; Jenssen, H.; Kindrachuk, J.; Fjell, C. D.; Korner, J.; Winkler, D. F. H.; Weaver, L. L.; Henklein, P.; Ulrich, A. S.; Chiang, S. H. Y.; Farmer, S. W.; Pante, N.; Volkmer, R.; Hancock, R. E. W. Screening and Characterization of Surface-Tethered Cationic Peptides for Antimicrobial Activity. *Chem. Biol.* **2009,** *16*, 58-69.
24. Wei, T.; Tang, Z. C.; Yu, Q.; Chen, H. Smart Antibacterial Surfaces with Switchable Bacteria-Killing and Bacteria-Releasing Capabilities. *ACS Appl. Mater. Interfaces* **2017,** *9*, 37511-37523.
25. Yan, S. J.; Shi, H. C.; Song, L. J.; Wang, X. H.; Liu, L.; Luan, S. F.; Yang, Y. M.; Yin, J. H. Nonleaching Bacteria-Responsive Antibacterial Surface Based on a Unique Hierarchical. *ACS Appl. Mater. Interfaces* **2016,** *8*, 24471-24481.
26. Lee, H.; Dellatore, S. M.; Miller, W. M.; Messersmith, P. B., Mussel-Inspired Surface Chemistry for Multifunctional Coatings. *Science* **2007**, *318*, 426-430.
27. Lou, T.; Bai, X. Q.; He, X. Y.; Yuan, C. Q., Antifouling Performance Analysis of Peptide-Modified Glass Microstructural Surfaces. *Appl. Surf. Sci.* **2021**, *541*, article No. 148384.
28. Cao, P.; Du, C. W.; He, X. Y.; Zhang, C.; Yuan, C. Q., Modification of a Derived Antimicrobial Peptide on Steel Surface for Marine Bacterial Resistance. *Appl. Surf. Sci.* **2020**, *510*, article No. 145512.
29. Cao, P.; Liu, K. W.; Liu, X. D.; Sun, W.; Wu, D. L.; Yuan, C. Q.; Bai, X. Q.; Zhang, C., Antibacterial Properties of Magainin II Peptide onto 304 Stainless Steel Surfaces: A Comparison Study of Two Dopamine Modification Methods. *Colloid Surf. B-Biointerfaces* **2020**, *194*, article No. 111198.
30. Lim, K. Y.; Chua, R. R. Y.; Bow, H.; Tambyah, P. A.; Hadinoto, K.; Leong, S. S. J., Development of a Catheter Functionalized by a Polydopamine Peptide Coating with Antimicrobial and Antibiofilm Properties. *Acta Biomater.* **2015,** *15*, 127-138.
31. Xu, D. W.; Yang, W. H.; Hu, Y.; Luo, Z.; Li, J. H.; Hou, Y. H.; Liu, Y.; Cai, K. Y., Surface Functionalization of Titanium Substrates with Cecropin B to Improve Their Cytocompatibility and Reduce Inflammation Responses. *Colloid Surf. B-Biointerfaces* **2013**, *110*, 225-235.
32. Tan, X. W.; Goh, T. W.; Saraswathi, P.; Nyein, C. L.; Setiawan, M.; Riau, A.; Lakshminarayanan, R.; Liu, S. P.; Tan, D.; Beuerman, R. W.; Mehta, J. S., Effectiveness of Antimicrobial Peptide Immobilization for Preventing Perioperative Cornea Implant-Associated Bacterial Infection. *Antimicrob. Agents Chemother.* **2014**, *58*, 5229-5238.
33. Shalev, T.; Gopin, A.; Bauer, M.; Stark, R. W.; Rahimipour, S., Non-leaching Antimicrobial Surfaces through Polydopamine Bio-inspired Coating of Quaternary Ammonium Salts or an Ultrashort Antimicrobial Lipopeptide. *J. Mater. Chem.* **2012**, 22, 2026-2032.
34. Yu, Q.; Wu, Z. Q.; Chen, H., Dual-function Antibacterial Surfaces for Biomedical Applications. *Acta Biomater.* **2015,** *16*, 1-13.
35. Mao, S. H.; Zhang, D.; He, X. M.; Yang, Y. T.; Protsak, I.; Li, Y. T.; Wang, J. W.; Ma, C. X.; Tan, J.; Yang, J. T., Mussel-Inspired Polymeric Coatings to Realize Functions from Single and Dual to Multiple Antimicrobial Mechanisms. *ACS Appl. Mater. Interfaces* **2021**, 13, 3089-3097.

36. Saha, A.; Nir, S.; Reches, M., Amphiphilic Peptide with Dual Functionality Resists Biofouling. *Langmuir* **2020,** *36*, 4201-4206.
37. Mei, Y.; Yu, K.; Lo, J. C. Y.; Takeuchi, L. E.; Hadjesfandiari, N.; Yazdani-Ahmadabadi, H.; Brooks, D. E.; Lange, D.; Kizhakkedathu, J. N. Polymer-Nanoparticle Interaction as a Design Principle in the Development of a Durable Ultrathin Universal Binary Antibiofilm Coating with Long-Term Activity. *ACS Nano* **2018,** *12*, 11881-11891.
38. Yu, K.; Alzahrani, A.; Khoddami, S.; Ferreira, D.; Scotland, K. B.; Cheng, J. T. J.; Ahmadabadi, H.Y.; Mei, Y.; Gill, A.; Takeuchi, L. E.; Yeung, E.; Grecov, D.; Hancock, R. E. W.;Chew, B.H.; Lange, D.; Kizhakkedathu, J.N. Self-limiting Mussel Inspired Thin Antifouling Coating with Broad Spectrum Resistance to Biofilm Formation to Prevent Catheter Associated Infection in Mouse and Porcine Models*, Adv. Healthcare Mater.* **2020**, article No. adhm.202001573.
39. von Gundlach, A.; Ashby, M. P.; Gani, J.; Lopez-Perez, P. M.; Cookson, A. R.; Huws, S. A.; Rumancev, C.; Garamus, V. M.; Mikut, R.; Rosenhahn, A.; Hilpert, K., BioSAXS Measurements Reveal That Two Antimicrobial Peptides Induce Similar Molecular Changes in Gram-Negative and Gram-Positive Bacteria. *Front. Pharmacol.* **2019**, 10, article No1127.
40. Wiegand, I.; Hilpert, K.; Hancock, R. E. W. Agar and Broth Dilution Methods to Determine the Minimal Inhibitory Concentration (MIC) of Antimicrobial Substances. *Nat. Protoc.* **2008,** *3*, 163-175.
41. Lau, K. H. A.; Ren, C. L.; Sileika, T. S.; Park, S. H.; Szleifer, I.; Messersmith, P. B., Surface-Grafted Polysarcosine as a Peptoid Antifouling Polymer Brush. *Langmuir* **2012,** *28*, 16099-16107.
42. Janssen, C.; Lo, J.; Jager, W.; Moskalev, I.; Law, A.; Chew, B. H.; Lange, D. A High Throughput, Minimally Invasive, Ultrasound Guided Model for the Study of Catheter Associated Urinary Tract Infections and Device Encrustation in Mice. *J. Urol.* **2014,** *192*, 1856-1863.
43. Yu, K.; Andruschak, P.; Yeh, H. H.; Grecov, D.; Kizhakkedathu, J. N., Influence of Dynamic Flow Conditions on Adsorbed Plasma Protein Corona and Surface-Induced Thrombus Generation on Antifouling Brushes. *Biomaterials* **2018**, 166, 79-95.
44. Hilpert, K.; Volkmer-Engert, R.; Walter, T.; Hancock, R.E.W. High-Throughput Generation of Small Antibacterial Peptides with Improved Activity *Nat. Biotechnol.* **2005**, *23*,1008-1012.
45. Yu, K.; Lai, B.F.L.; Gani, J.; Mikut, R.; Hilpert, K.; Kizhakkedathu, J.N. Interaction of Blood Components with Cathelicidins and Their Modified Versions, *Biomaterials* **2015**, *69*, 201-211.
46. Ryu, J. H.; Messersmith, P. B.; Lee, H. Polydopamine Surface Chemistry: A Decade of Discovery. *ACS Appl. Mater. Interfaces* **2018,** *10*, 7523-7540.
47. Gao, G. Z.; Lange, D.; Hilpert, K.; Kindrachuk, J.; Zou, Y. Q.; Cheng, J. T. J.; Kazemzadeh-Narbat, M.; Yu, K.; Wang, R. Z.; Straus, S. K.; Brooks, D. E.; Chew, B. H.; Hancock, R. E. W.; Kizhakkedathu, J. N. The Biocompatibility and Biofilm Resistance of Implant Coatings Based on Hydrophilic Polymer Brushes Conjugated with Antimicrobial Peptides. *Biomaterials* **2011,** *32*, 3899-3909.
48. Gao, G. Z.; Yu, K.; Kindrachuk, J.; Brooks, D. E.; Hancock, R. E. W.; Kizhakkedathu, J. N., Antibacterial Surfaces Based on Polymer Brushes: Investigation on the Influence of Brush Properties on Antimicrobial Peptide Immobilization and Antimicrobial Activity. *Biomacromolecules* **2011,** *12*, 3715-3727.

49. Bingen. P.; Wang, G.; Steinmetz, N.F.; Rodahl, M.; Richter, R.P. Solvation effects in the Quartz Crystal Microbalance with Dissipation Monitoring Response to Biomolecular Adsorption. A Phenomenological Approach. *Anal Chem.* **2008**, *80*, 8880-8890.
50. Hartmann, M.; Berditsch, M.; Hawecker, J.; Ardakani, M. F.; Gerthsen, D.; Ulrich, A. S., Damage of the Bacterial Cell Envelope by Antimicrobial Peptides Gramicidin S and PGLa as Revealed by Transmission and Scanning Electron Microscopy. *Antimicrob. Agents Chemother.* **2010,** *54*, 3132-3142.
51. Gao, G.; Cheng, J. T. J.; Kindrachuk, J.; Hancock, R. E. W.; Straus, S. K.; Kizhakkedathu, J. N. Biomembrane Interactions Reveal the Mechanism of Action of Surface-Immobilized Host Defense IDR-1010 Peptide. *Chem. Biol.* **2012**, *19*, 199-209.
52. Hilpert, K.; Elliott, M.R.; Volkmer-Engert, R.; Henklein, P.; Donini, O.; Zhou, Q.; Winkler, D.F.; and Hancock, R.E.W. Sequence Requirements and an Optimization Strategy for Short Antimicrobial Peptides. *Chem. Biol.* **2006**, *13*, 1101–1107.
53. Mansour, S. C.; de la Fuente-Nunez, C.; Hancock, R. E. W. Peptide IDR-1018: Modulating the Immune System and Targeting Bacterial Biofilms to Treat Antibiotic-Resistant Bacterial Infections. *J. Pept. Sci.* **2015,** *21*, 323-329.
54. Haney, E. F.; Brito-Sanchez, Y.; Trimble, M. J.; Mansour, S. C.; Cherkasov, A.; Hancock, R. E. W. Computer-aided Discovery of Peptides that Specifically Attack Bacterial Biofilms. *Sci Rep* **2018,** *8*, article No. 1871.
55. de la Fuente-Nunez, C.; Reffuveille, F.; Mansour, S. C.; Reckseidler-Zenteno, S. L.; Hernandez, D.; Brackman, G.; Coenye, T.; Hancock, R. E. W. D-Enantiomeric Peptides that Eradicate Wild-Type and Multidrug-Resistant Biofilms and Protect against Lethal Pseudomonas aeruginosa Infections. *Chem. Biol.* **2015,** *22*, 196-205.
56. Costa, F.; Carvalho, I. F.; Montelaro, R. C.; Gomes, P.; Martins, M. C. L. Covalent Immobilization of Antimicrobial Peptides (AMPs) onto Biomaterial Surfaces. *Acta Biomater.* **2011,** *7*, 1431-1440.
57. Xiao, M. Y.; Jasensky, J.; Foster, L.; Kuroda, K.; Chen, Z. Monitoring Antimicrobial Mechanisms of Surface-Immobilized Peptides in Situ. *Langmuir* **2018,** *34*, 2057-2062.
58. Zhang, X. Y.; Zhao, Y. Q.; Zhang, Y. D.; Wang, A. Z.; Ding, X. K.; Li, Y.; Duan, S.; Ding, X. J.; Xu, F. J. Antimicrobial Peptide-Conjugated Hierarchical Antifouling Polymer Brushes for Functionalized Catheter Surfaces. *Biomacromolecules* **2019,** *20*, 4171-4179.
59. Yan, S. J.; Shi, H. C.; Song, L. J.; Wang, X. H.; Liu, L.; Luan, S. F.; Yang, Y. M.; Yin, J. H. Nonleaching Bacteria-Responsive Antibacterial Surface Based on a Unique Hierarchical Architecture. *ACS Appl. Mater. Interfaces* **2016**, *8*, 24471-24481.
60. Sundaram, H. S.; Ella-Menye, J. R.; Brault, N. D.; Shao, Q.; Jiang, S. Y. Reversibly Switchable Polymer with Cationic/Zwitterionic/Anionic Behavior through Synergistic Protonation and Deprotonation. *Chem. Sci.* **2014,** *5*, 200-205.
61. Liu, S. Q.; Yang, C.; Huang, Y.; Ding, X.; Li, Y.; Fan, W. M.; Hedrick, J. L.; Yang, Y. Y. Antimicrobial and Antifouling Hydrogels Formed In Situ from Polycarbonate andPoly(ethylene glycol) via Michael Addition. *Adv. Mater.* **2012,** *24*, 6484-6489.
62. Liu, C. Y.; Huang, C. J. Functionalization of Polydopamine via the Aza-Michael Reaction for Antimicrobial Interfaces. *Langmuir* **2016,** *32*, 5019-5028.
63. Fan, Y. J.; Pham, M. T.; Huang, C. J. Development of Antimicrobial and Antifouling Universal Coating via Rapid Deposition of Polydopamine and Zwitterionization. *Langmuir* **2019,** *35*, 1642-1651.

64. Sileika, T. S.; Kim, H. D.; Maniak, P.; Messersmith, P. B. Antibacterial Performance of Polydopamine-Modified Polymer Surfaces Containing Passive and Active Components. *ACS Appl. Mater. Interfaces* **2011,** *3*, 4602-4610.
65. Cheng, W.; Zeng, X. W.; Chen, H. Z.; Li, Z. M.; Zeng, W. F.; Mei, L.; Zhao, Y. L. Versatile Polydopamine Platforms: Synthesis and Promising Applications for Surface Modification and Advanced Nanomedicine. *ACS Nano* **2019,** *13*, 8537-8565.
66. Lai, B. F. L.; Creagh, A. L.; Janzen, J.; Haynes, C. A.; Brooks, D. E.; Kizhakkedathu, J. N. The Induction of Thrombus Generation on Nanostructured Neutral Polymer Brush Surfaces. *Biomaterials* **2010,** *31*, 6710-6718.
67. Weiser, A. A.; Or-Guil, M.; Tapia, V.; Leichsenring, A.; Schuchhardt, J.; Frommel, C.; Volkmer-Engert, R. SPOT Synthesis: Reliability of Array-Based Measurement of Peptide Binding Affinity. *Anal. Biochem.* **2005,** *342*, 300-311.

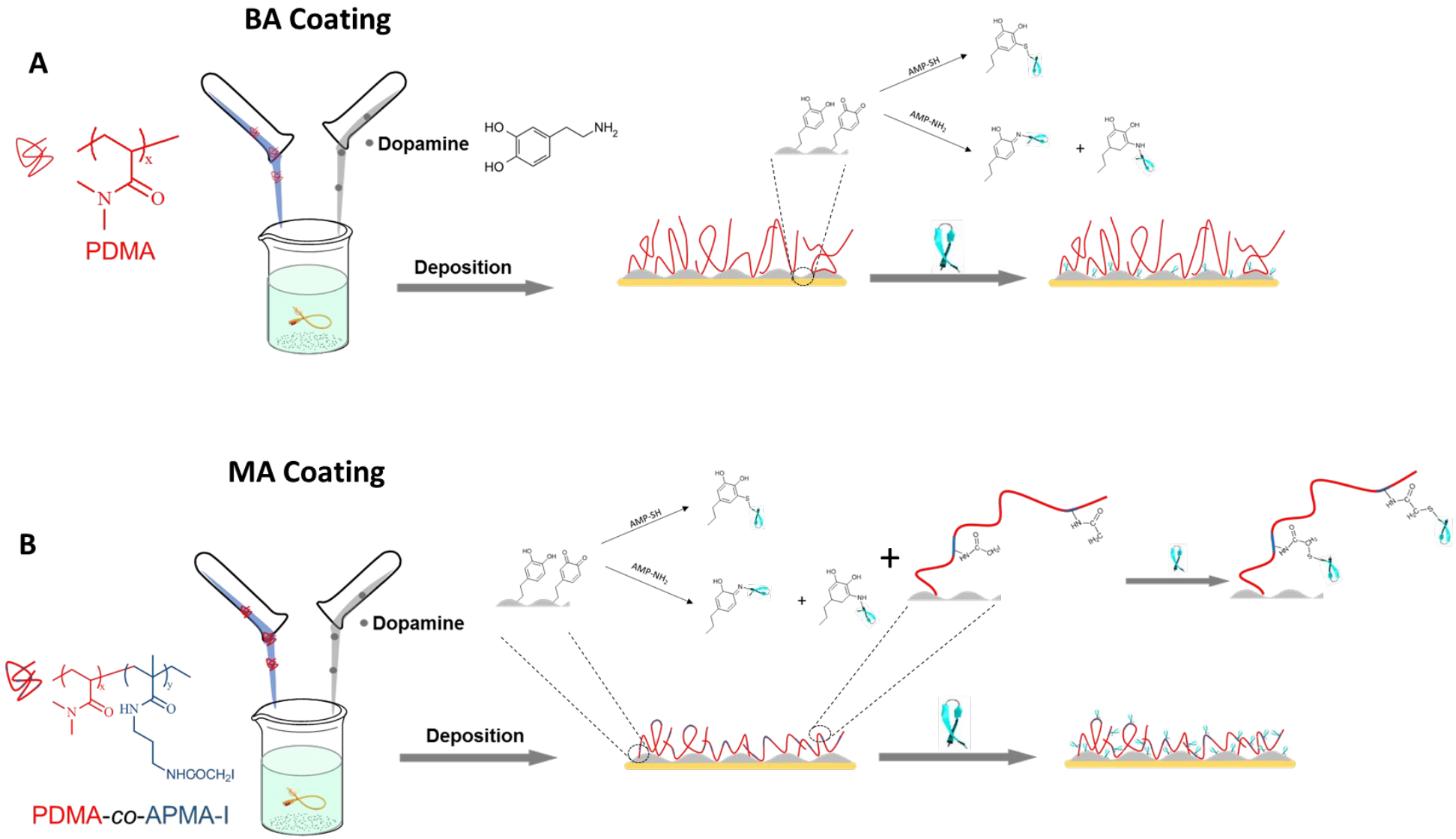

Figure 1. **Schematic representation of conjugation of AMPs onto non-fouling coating with different structure of polymer chains on the surface.** (**A**) Conjugation of AMPs directly onto PDA component in a non-fouling background generated by PDA/PDMA coating (BA coating). The AMPs were conjugated by the reaction between quinone groups in the underlying PDA and amine or thiol groups in the AMP. (**B**) Conjugation of AMPs via a copolymer approach (MA coating). The AMPs was tethered into the coating between the reaction of iodoacetamide groups on the polymers and thiol groups on the AMP as well as the reaction between PDA and AMP

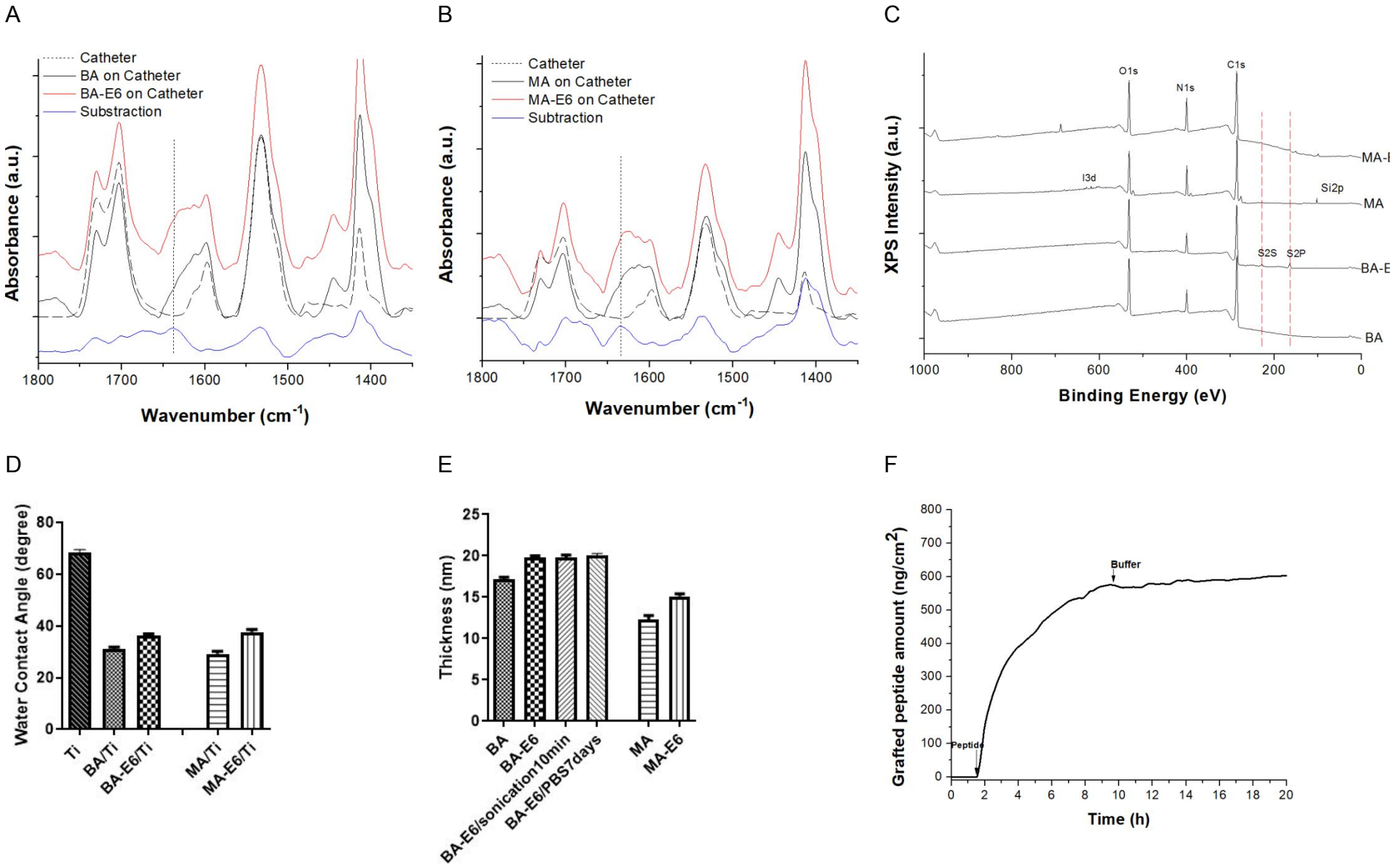

Figure 2. Surface characterization of the coatings. (A) ATR-FTIR spectra of BA coating on 14G catheter before and after peptide conjugation and the spectral subtraction. (B) ATR-FTIR spectra of MA coating on 14G catheter before and after peptide conjugation.

(C) XPS survey scan of BA and MA coatings on silicon wafer before and after peptide conjugation. The change in water angle (D) and thickness (E) of the coating on Ti substrate before and after peptide conjugation. (F) Coating stability. The unnoticeable change in thickness of the coating indicates that it is stable in PBS for 7 days and can withstand ultrasonication for 10 min. (F) QCM-D real-time analysis of the conjugation of E6 to the BA-coated surface in buffer (pH 8.0).

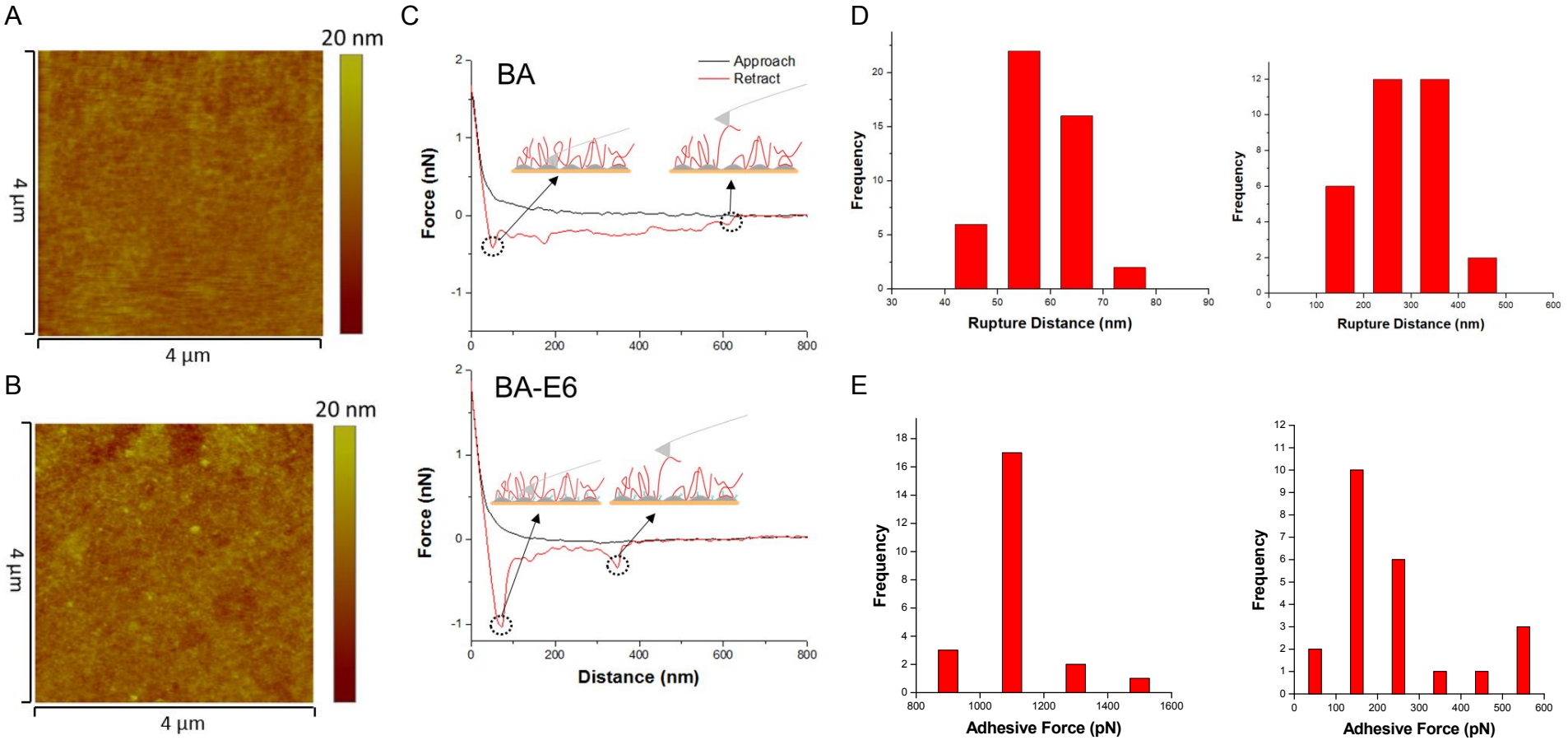

Figure 3. **Surface characterization via atomic force microscopy.** Surface morphology of BA (A) and BA-E6 (B) coating on Silicon wafer. AFM force spectroscopy of (C) BA coating and BA-E6 coating on silicon wafer. Representative approach (black line) and retraction (red line) force curves are shown. Distribution of the (D) rupture distance and (E) the corresponding adhesive force for the BA-E6 coated silicon wafer.

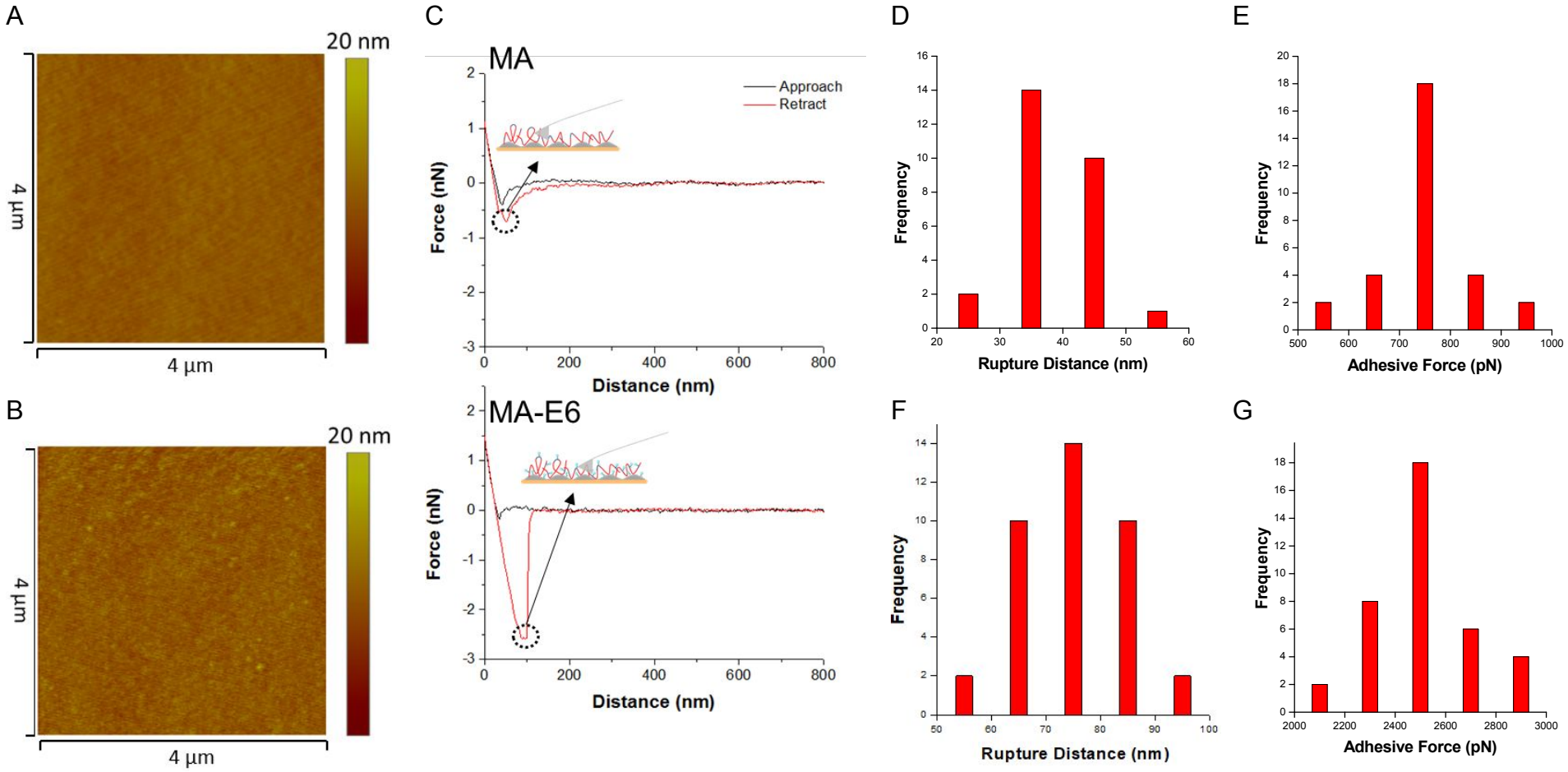

Figure 4. **Surface characterization via atomic force microscopy.** Surface morphology of MA (A) and MA-E6 (B) coating on Silicon wafer. AFM force spectroscopy of (C) MA coating and MA-E6 coating on silicon wafer. Representative approach (black line) and retraction (red line) force curves are shown. Distribution of (D) rupture distance and (E) adhesive force for the MA coating on silicon wafer. Distribution of the (F) rupture distance and (G) adhesive force for the MA-E6 coating on silicon wafer.

A Ti BA BA-E6 MA MA-E6

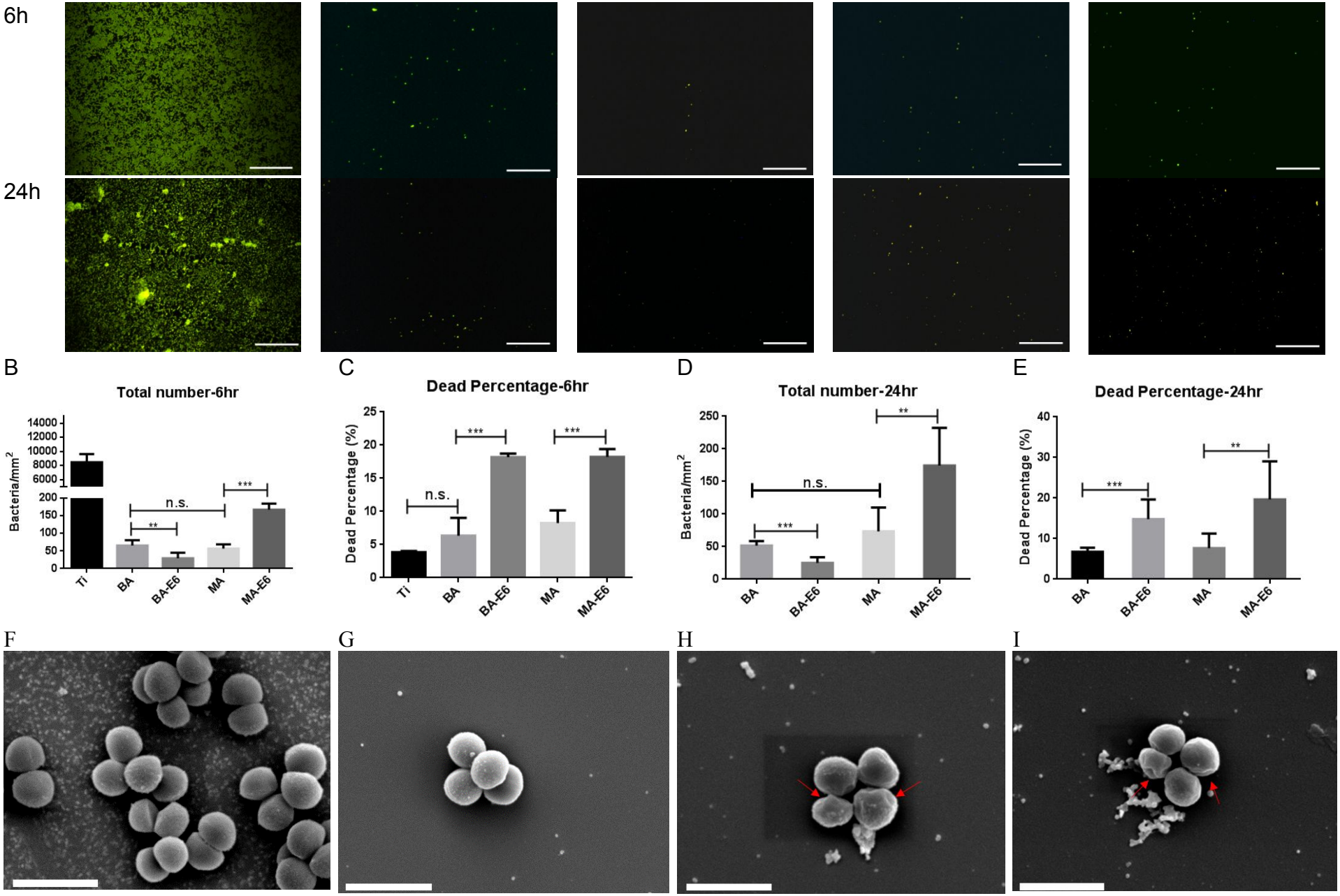

Figure 5. Efficiency of coatings in prevention of early-stage biofilm formation. Ti coated silicon wafers were used for the study. Representative fluorescence microscopy images of bacterial adhesion *(S. saprophyticus)* on (A) uncoated Ti, BA, BA-E6, MA and MA-

E6 coatings after 6h and 24 h incubation in TSB medium. Number and percentage of dead bacteria adhered onto the bare Ti substrate and on different coatings at 6 h (B and C) and 24 h (D and E). Scale bar = 100 μm. The morphology of bacteria adhered to the (F) uncoated Ti, (G) BA, (H) BA-E6 and (I) MA-E6 coatings. Scale bar = 2 μm. Approximately 5 x 10^5 CFU/mL (1ml) were added to each sample in a 24 wells plate and incubated at 37 ºC on a platform rocking at 50 rpm. Student's two-tailed unpaired t-test was used for statistical analysis (N = 3). *. $p \leq 0.05$, **, $p \leq 0.01$, and ***. $p \leq 0.001$.

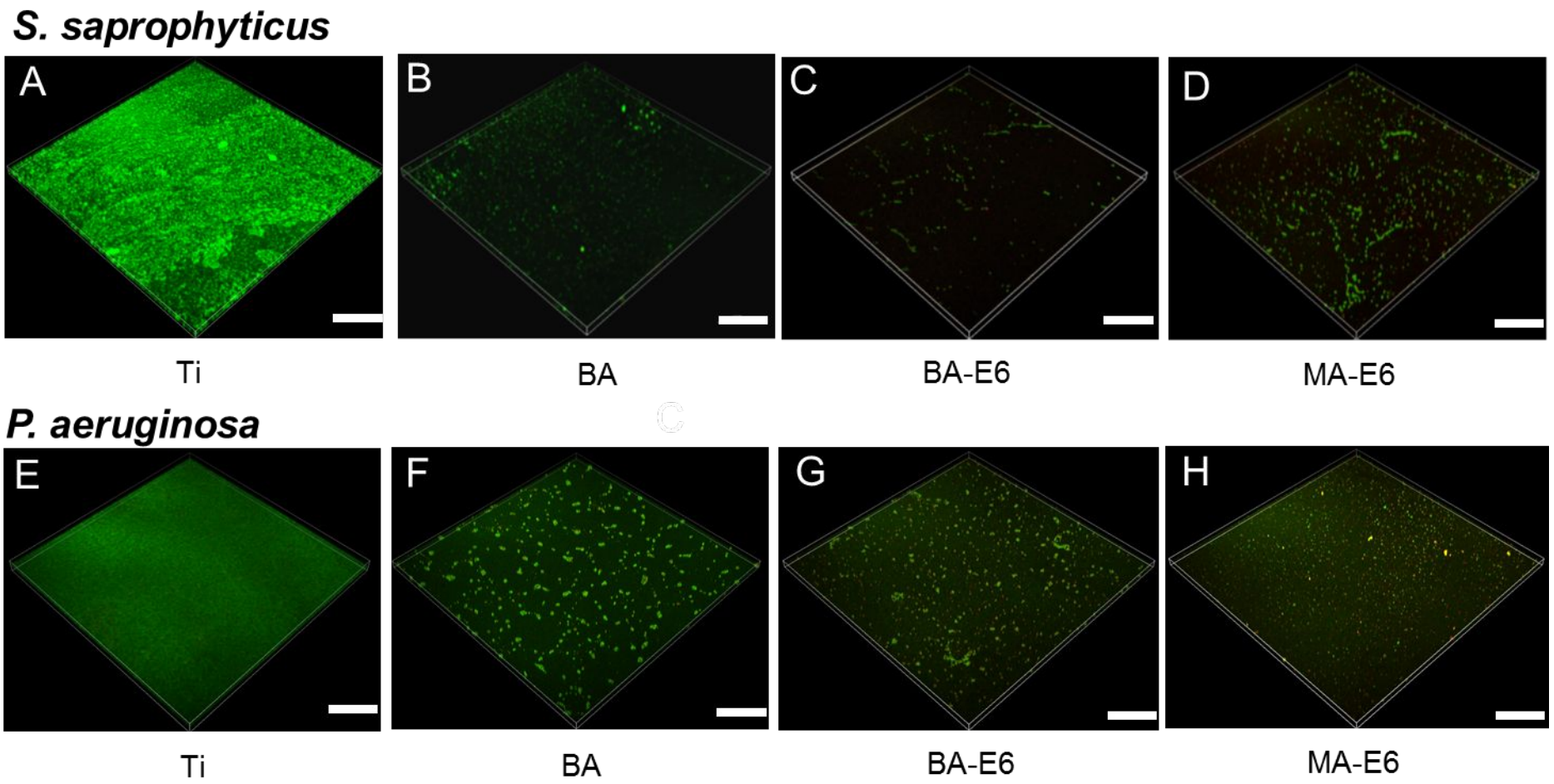

Figure 6. **Efficiency in prevention of biofilm formation *in vitro* by different coatings**. Representative confocal fluorescence microscopy images of *S. saprophyticus* biofilm formation on (A) uncoated Ti, (B) BA coating, (C) BA-E6 coating and (D) MA-E6 coating. Representative confocal fluorescence microscopy images of *P. aeruginosa* biofilm formation on (E) uncoated Ti, (F) BA coating, (G) BA-E6 coating and (H) MA-E6 coating. Scale bar = 100 µm. 1 mL bacterial culture with initial count of ~5 x 10^5 CFU/mL was added to each sample in the wells of 24 wells plate and incubated at 37ºC on a platform rocking at 50 rpm for 24 h

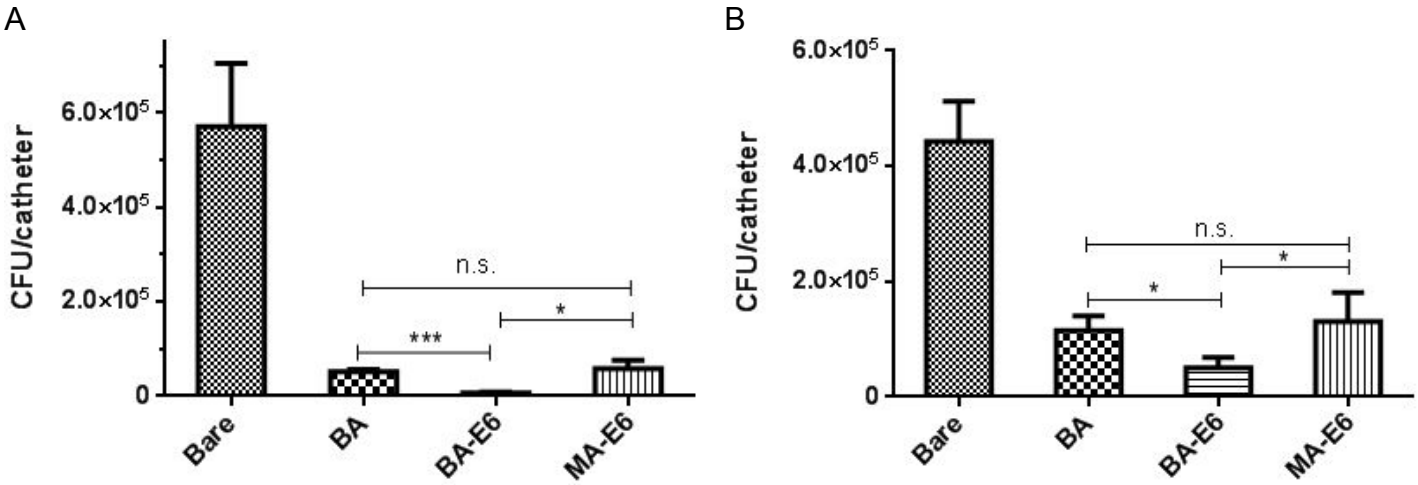

Figure 7. Efficiency in prevention of biofilm formation *in vitro*. (A) The reduction of bacterial adhesion (*S. saprophyticus*) on coated 14G PU catheter after incubation in TSB medium for 24h. (B) The reduction of bacterial adhesion (*P. aeruginosa*) on coated 14G PU catheter after incubation in LB medium for 24 h. Student's two-tailed unpaired t-test was used for statistical analysis (N = 3). *. $p < 0.05$; ** $p < 0.01$; ***, $p < 0.001$.

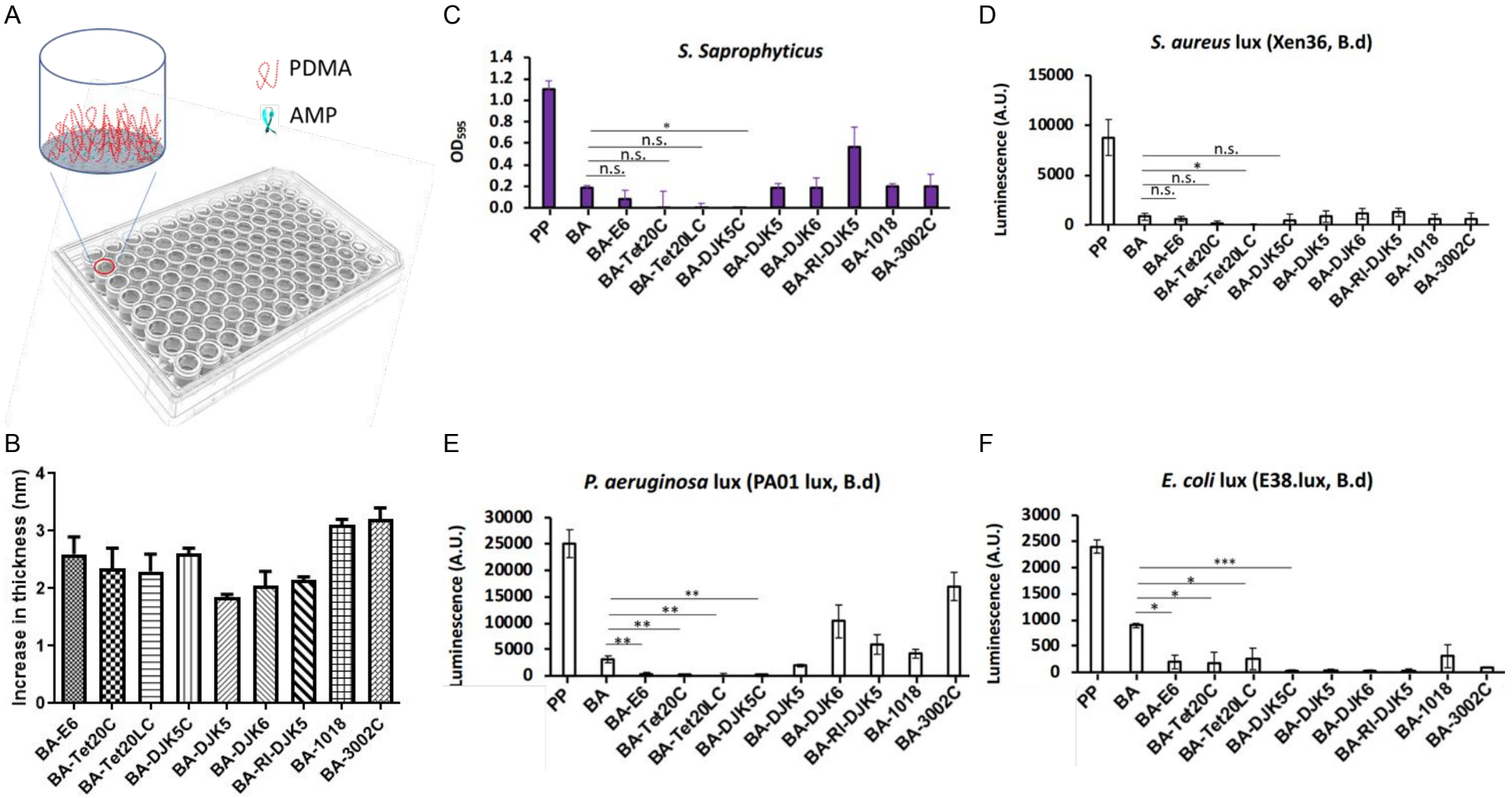

Figure 8. **Semi-throughput screening method for the identification of high efficiency antibiofilm surface immobilized peptides in relevant non-fouling background.** (A) Schematic of BA-AMP coating on 96 wells plate. Different from the conventional tethered AMPs on the substrate, the AMPs in the BA-AMP coating is presented in a non-fouling background generated by PDMA chains. (B) Increase in thickness after peptide conjugation on the BA coating modified silicon substrate. Screening of tethered peptides utilizing BA-AMP coating against *S. saprophyticus* (C), *S. aureus* (D), *P. aeruginosa* (E) and *E. coli* (F). Student's two-tailed unpaired t-test was used for statistical analysis (N = 3). n.s.: not significant difference. *. $p < 0.05$; ** $p < 0.01$; ***, $p < 0.001$.

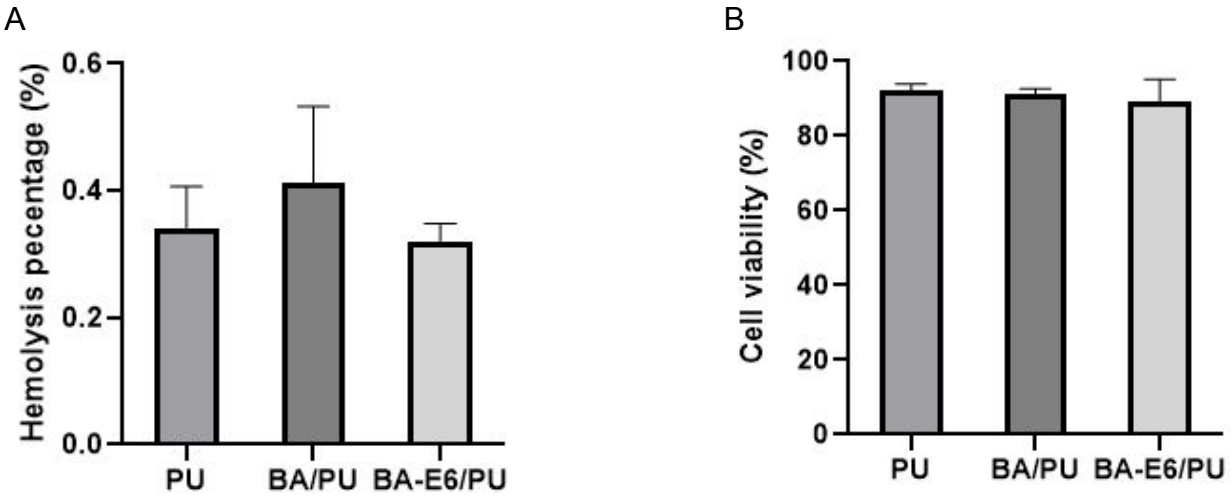

Figure 9. **Hemolysis and cytocompatibility of BA and BA-E6 coating on PU surfaces**. (A) Percentage of hemolysis triggered by the BA and BA-E6 coated PU coupon (diameter of 5/8"), (B) Viability of T24 cells grown on the BA and BA-E6 coated PU coupon.

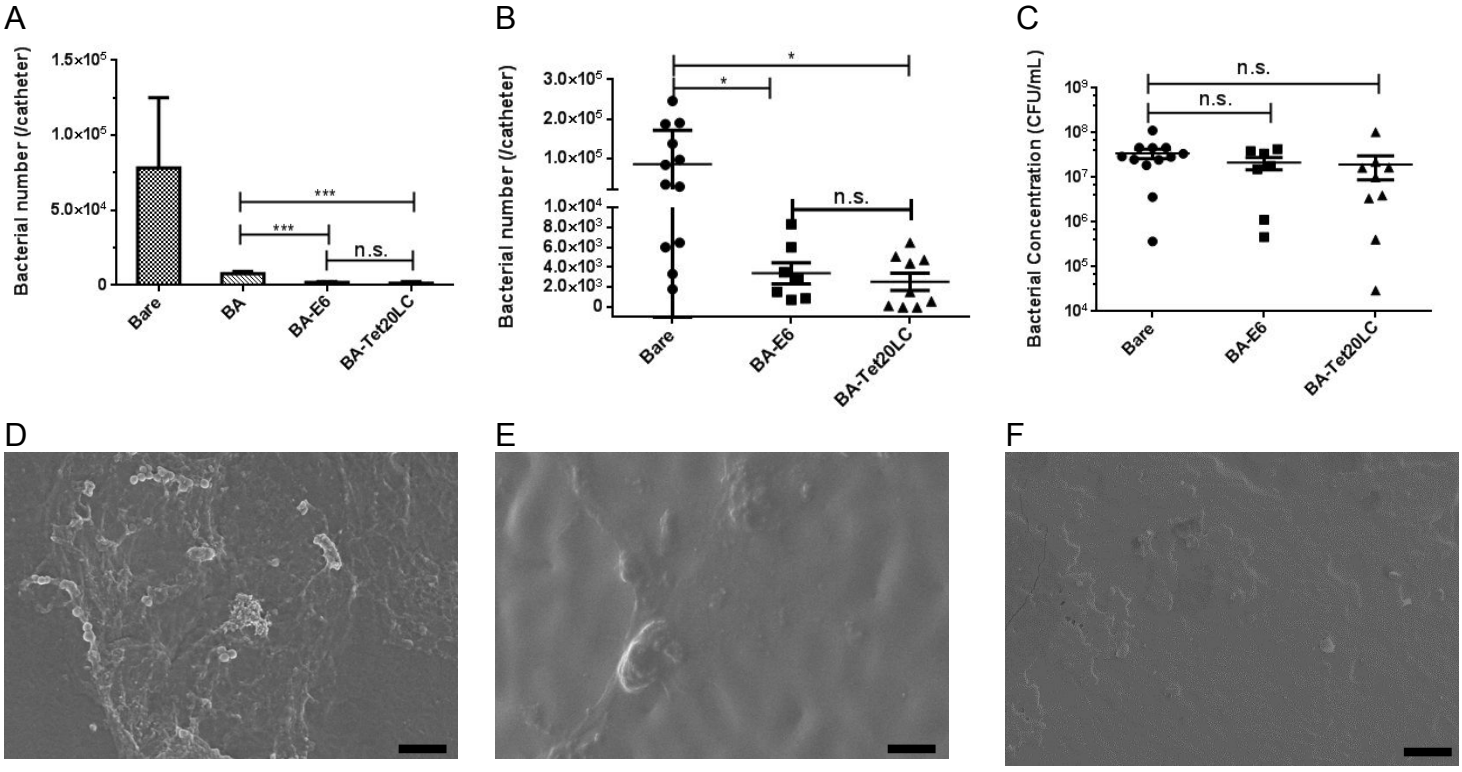

Figure 10. Inhibition of biofilm formation by *S. saprophyticus* by the BA coating conjugated with E6 or Tet20LC on PU catheters *in vitro* and in mouse urinary tract infection model. (A) Number of survived *S. saprophyticus* recovered from the 24G PU catheter surface after incubating for 24 h *in vitro*. (B) Number of *S. saprophyticus* adhered on the PU catheter surface and (C) in the urine after 7 days *in vivo* in urinary infection model. SEM images of biofilm on (D) bare and (E) BA coating conjugated with E6, (F) Tet20LC coated catheter after instillation in mice for 7 days. (Scale bar = 5 μm). N = 12 mice for the control (pristine PU catheter), N = 7 mice for the BA-E6 coated catheter and N = 9 mice for the BA-Tet20LC coated catheter. Student's two-tailed unpaired t-test was used for statistical analysis. * indicates $p \leq 0.05$, *** indicates $p \leq 0.001$.

Table 1. Surface elemental composition of the coating on silicon wafer substrate from XPS analysis

	Si	PDA/Si	BA/Si	BA-E6/Si	MA/Si	MA-E6/Si
C%	9.3	74.4	72	68.4	67.8	67.9
N%	1.2	6.9	9.7	9.9	10.8	13.7
O%	39.5	18.2	17.9	19.5	18.2	15.1
Si%	50	0.5	0.4	0	3.2	1.6
S%	0	0	0	2.2	0	1.8
I%	0	0	0	0	0.1	0

Table 2. Antimicrobial peptides, their sequences and minimal inhibition concentration (MIC) used in this study. All peptides were amidated at the C-terminus and lower case letters refer to D-amino acids.

AMPs	**Sequence**	MIC (μg/mL)				Grafting density (ng/cm^2)
		P. aeruginosa	***E. coli***	***S. aureus***	***S. saprophyticus***	
E6	RRWRIVVIRVRRC	32	8	64	4	312 ± 36
Tet20C	KRWRIRVRVIRKC	8	4	64	2	282 ± 42
Tet20LC	KRWRIRVRVIRK-bA-bA-C	16	4	64	2	276 ± 36
DJK5C	Vqwrairvrvirc	16	4	16	2	312 ± 12
DJK5	Vqwrairvrvir	16	1.6	16	2	222 ± 12
IDR-1018	VRLIVAVRIWRR	64	9.3	16	2	372 ± 12
3002C	ILVRWIRWRIQWC	128	16	32	8	384 ± 24

Table of Contents